

*Chaos: from Simple Models to Complex Systems,*

(World Scientific, Singapore, 2009)

ISBN: 978-981-4277-65-5

## **SOLUTION TO EXERCISES**

(Dated: September 14, 2009)

## CHAPTER 2: The Language of Dynamical Systems

### Exercise 2.1

Consider the following systems and specify whether: A) chaos can or cannot be present; B) the system is conservative or dissipative.

1. 
$$\begin{aligned}x(t+1) &= x(t) + y(t) && \text{mod } 1 \\y(t+1) &= 2x(t) + 3y(t) && \text{mod } 1;\end{aligned}$$

2. 
$$x(t+1) = \begin{cases} x(t) + 1/2 & x(t) \in [0:1/2] \\ x(t) - 1/2 & x(t) \in [1/2:1] \end{cases}$$

3. 
$$\frac{dx}{dt} = y, \quad \frac{dy}{dt} = -\alpha y + f(x - \omega t), \quad \text{where } f \text{ is a periodic function, and } \alpha > 0.$$

### Solution

The system 1) is conservative as its Jacobian matrix

$$\mathbb{L} = \begin{pmatrix} 1 & 1 \\ 2 & 3 \end{pmatrix}$$

has determinant 1. Moreover, the eigenvalues of  $\mathbb{L}$  are  $\lambda_{1,2} = 2 \pm \sqrt{3}$ . As at least one of them has modulus  $> 1$ , the system is chaotic.

The system 2) cannot be chaotic as  $|f'| = 1$ , moreover the system is conservative  $\delta x(t+1) = \delta x(t)$ .

The linear stability matrix of the ODE 3) is

$$\mathbb{L} = \begin{pmatrix} 0 & 1 \\ f'(x - \omega t) & -\alpha \end{pmatrix}$$

and being its trace negative, i.e.  $\text{Tr}[\mathbb{L}] = -\alpha < 0$ , the system is dissipative. By introducing the new variable  $z = x - \omega t$ , the system takes the form

$$\begin{aligned}\frac{dz}{dt} &= y + \omega \\ \frac{dy}{dt} &= -\alpha y + f(z)\end{aligned}$$

which is an autonomous two-dimensional system. Therefore, by invoking the Poincaré-Bendixon theorem (Sec. 2.3), we can conclude that the system can evolve only towards fixed points or limit cycles so that chaos can never appear.

### Exercise 2.2

*Find and draw the Poincaré section for the forced oscillator*

$$\frac{dx}{dt} = y, \quad \frac{dy}{dt} = -\omega x + F \cos(\Omega t),$$

with  $\omega^2 = 8$ ,  $\Omega = 2$  and  $F = 10$ .

### Solution

The solution of the forced oscillator is

$$\begin{aligned}x(t) &= A \sin(\sqrt{\omega}t + \phi) + \frac{F}{\omega - \Omega^2} \left( \cos(\Omega t) - \cos(\sqrt{\omega}t) \right) \\ y(t) &= A\omega \cos(\sqrt{\omega}t + \phi) - \frac{F}{\omega - \Omega^2} \left( \Omega \sin(\Omega t) - \sqrt{\omega} \sin(\sqrt{\omega}t) \right)\end{aligned}$$

where we assigned the initial conditions  $x(0) = X_0, y(0) = V_0$ , setting the constants  $A \sin(\phi) = X_0$  and  $\tan(\phi) = \sqrt{\omega}X_0/V_0$ . To compute the Poincaré section we can select discrete times  $\Omega t_n = 2\pi n$  where the motion is evaluated  $(x(n), y(n)) = (x(t_n), y(t_n))$ ,

$$\begin{aligned}x(n) &= A \sin(qn + \phi) + \frac{F[1 - \cos(qn)]}{\omega - \Omega^2} \\ y(n) &= \sqrt{\omega}A \cos(qn + \phi) + \frac{F\sqrt{\omega} \sin(qn)}{\omega - \Omega^2}\end{aligned}$$

where  $q = 2\pi\sqrt{\omega}/\Omega$ . If the ratio  $\sqrt{\omega}/\Omega$  is rational the section is made of isolated points in the  $x, y$ -plane (periodic motion), if the ratio is irrational the motion is quasiperiodic and the section is a closed line in the plane  $x, y$ .

### Exercise 2.3

Consider the following periodically forced system,

$$\frac{dx}{dt} = y, \quad \frac{dy}{dt} = -\omega x - 2\mu y + F \cos(\Omega t).$$

Convert it in a three-dimensional autonomous system and compute the divergence of the vector field, discussing the conservative and dissipative condition.

#### Solution

Introducing the auxiliary variable  $z = \Omega t$ , the system becomes a three-dimensional autonomous ODE  $d\mathbf{r}/dt = \mathbf{F}(\mathbf{r})$  ( $\mathbf{r} = (x, y, z)$ )

$$\begin{aligned} \frac{dx}{dt} &= y \\ \frac{dy}{dt} &= -\omega x - 2\mu y + F \cos(z) \\ \frac{dz}{dt} &= \Omega \end{aligned}$$

whose divergence is

$$\nabla \cdot \mathbf{F} = -2\mu.$$

The system is thus dissipative for  $\mu > 0$  and conservative for  $\mu = 0$ . The condition  $\mu < 0$  is unphysical as implies indefinite expansion of the system.

### Exercise 2.4

Show that in a system satisfying Liouville theorem,  $dx_n/dt = f_n(\mathbf{x})$ , with  $\sum_{n=1}^N \partial f_n(\mathbf{x})/\partial x_n = 0$ , asymptotic stability is impossible.

#### Solution

To prove the statement it is sufficient to observe that given a set  $\Omega_0$  of positive volume  $\text{Vol}(\Omega_0) = V_0 > 0$ , then for the set  $\Omega_t$  containing the evolution  $\mathbf{x}(t)$  of the point  $\mathbf{x}_0 \in \Omega_0$ , one has  $\text{Vol}(\Omega_t) = \text{const}$ . While the condition of asymptotic stability would require the convergence of all trajectories to the fixed point, and thus the asymptotic contraction of volumes in phase space.

### Exercise 2.5

Discuss the qualitative behavior of the following ODEs

$$1. \quad \frac{dx}{dt} = x(3 - x - y), \quad \frac{dy}{dt} = y(x - 1)$$

$$2. \quad \frac{dx}{dt} = x^2 - xy - x, \quad \frac{dy}{dt} = y^2 + xy - 2y$$

### Solution

The qualitative analysis generally begins with the identification of the fixed (critical) points.

1) To identify the fixed points of the first system, we need to solve simultaneously the two equations:

$$x(3 - x - y) = 0 \quad y(x - 1) = 0,$$

which have three solutions (fixed points)  $P_0 = (0, 0)$ ,  $P_1 = (1, 2)$  and  $P_2 = (3, 0)$ . The stability analysis determines the local behaviour of the system trajectories around each of the fixed points.

The stability matrices of each point are:

$$\mathbb{L}_0 = \begin{pmatrix} 3 & 0 \\ 0 & -1 \end{pmatrix}, \quad \mathbb{L}_1 = \begin{pmatrix} 1 & -1 \\ 2 & 0 \end{pmatrix}, \quad \mathbb{L}_2 = \begin{pmatrix} -3 & -3 \\ 0 & 2 \end{pmatrix}.$$

Accordingly the point  $P_0$  is a saddle as the  $\mathbb{L}_0$  has eigenvalues  $\lambda_1 = 3, \lambda_2 = -1$ . The eigenvectors  $\mathbf{e}_1 = (1, 0)$   $\mathbf{e}_2 = (0, 1)$  determine the directions of the motion around  $P_0$ .

The solutions of the system around  $P_0$  in the linear approximation are:

$$\begin{pmatrix} \delta x(t) \\ \delta y(t) \end{pmatrix} = \begin{pmatrix} 1 \\ 0 \end{pmatrix} \exp(3t) + \begin{pmatrix} 0 \\ 1 \end{pmatrix} \exp(-2t)$$

contract along the direction  $\mathbf{e}_2 = (0, 1)$  and expand along  $\mathbf{e}_1 = (1, 0)$ .

The point  $P_1$  is a stable spiral as its stability matrix  $\mathbb{L}_1$  has a couple of complex conjugated eigenvalues  $\lambda_1 = -(1 - i\sqrt{7})/4, \lambda_2 = -(1 + i\sqrt{7})/4$  associated to the complex eigenvectors  $\mathbf{e}_1 = (\lambda_1, 1)$ ,  $\mathbf{e}_2 = (\lambda_2, 1)$ . The behaviour of the system around  $P_1$  is a spiral motion towards  $P_1$  in anticlockwise sense.

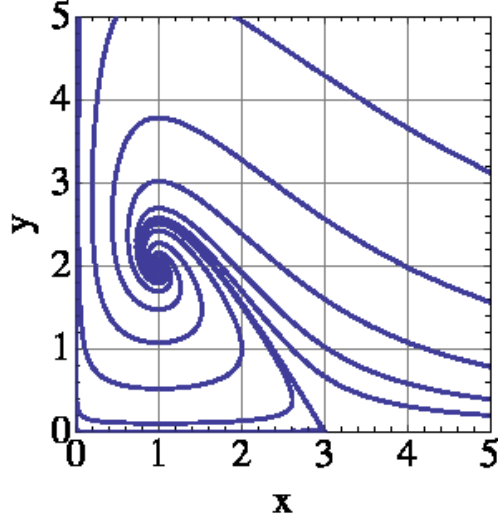


FIG. 1: Spiralling behavior of the trajectories around fixed point  $P_1$ .

The point  $P_2$  is a saddle, indeed its stability matrix  $\mathbb{L}_1$  has eigenvalues  $\lambda_1 = -3, \lambda_2 = 2$ , and eigenvectors  $\mathbf{e}_1 = (1, 0)$ ,  $\mathbf{e}_2 = (-3, 5)$ . The behaviour of the system around  $P_2$  is given by the solution of the linearized problem

$$\begin{pmatrix} \delta x(t) \\ \delta y(t) \end{pmatrix} = \begin{pmatrix} 1 \\ 0 \end{pmatrix} \exp(-3t) + \begin{pmatrix} -3 \\ 5 \end{pmatrix} \exp(2t)$$

Having identified the behavior of trajectories around the fixed points it is now rather easy to sketch the qualitative behavior in phase space which looks like in Fig.1.

2) Analogously to the previous system, the fixed points are obtained from

$$\begin{aligned} x^2 - xy - x &= 0 \\ y^2 + xy - 2y &= 0 \end{aligned}$$

whose solution are  $P_0 = (0, 0)$ ,  $P_1 = (0, 2)$ ,  $P_2 = (1, 0)$  and  $P_3 = (3/2, 1/2)$ . The linear stability analysis requires to compute the stability matrices for each of the fixed points

$$\mathbb{L}_0 = \begin{pmatrix} -1 & 0 \\ 0 & -2 \end{pmatrix}, \quad \mathbb{L}_1 = \begin{pmatrix} -3 & 0 \\ 2 & 2 \end{pmatrix}, \quad \mathbb{L}_2 = \begin{pmatrix} 1 & -1 \\ 0 & -1 \end{pmatrix}, \quad \mathbb{L}_3 = \begin{pmatrix} 1/2 & -1 \\ 1/2 & 0 \end{pmatrix}.$$

From the eigenvalues and eigenvectors of these matrices we can deduce the stability and the behavior of the solution in a sufficiently small neighborhood of the fixed points, which is typically enough to have a qualitative idea of the system dynamics.

The point  $P_0$  is stable, as it corresponds to eigenvalues  $\lambda_1 = -2, \lambda_2 = -1$  associated to eigenvectors  $\mathbf{e}_1 = (0, 1), \mathbf{e}_2 = (1, 0)$ . Therefore, around  $P_0$ , the trajectories exponentially approach  $P_0$  as

$$\begin{pmatrix} \delta x(t) \\ \delta y(t) \end{pmatrix} = \begin{pmatrix} 0 \\ 1 \end{pmatrix} \exp(-2t) + \begin{pmatrix} -3 \\ 5 \end{pmatrix} \exp(-t) .$$

The points  $P_1$  and  $P_2$  are saddles (hyperbolic points). Indeed  $\mathbb{L}(P_1)$  has eigenvalues  $\lambda_1 = -3, \lambda_2 = 2$  and eigenvectors  $\mathbf{e}_1 = (-5, 2), \mathbf{e}_2 = (0, 1)$  so that

$$\begin{pmatrix} \delta x(t) \\ \delta y(t) \end{pmatrix} = c_1 \begin{pmatrix} 5 \\ -2 \end{pmatrix} \exp(-3t) + c_2 \begin{pmatrix} 0 \\ 1 \end{pmatrix} \exp(2t) .$$

Similarly, around  $P_2$

$$\begin{pmatrix} \delta x(t) \\ \delta y(t) \end{pmatrix} = c_1 \begin{pmatrix} 1 \\ 2 \end{pmatrix} \exp(-t) + c_2 \begin{pmatrix} 1 \\ 0 \end{pmatrix} \exp(t) ,$$

indeed  $\lambda_1 = -1, \lambda_2 = 1$ , and  $\mathbf{e}_1 = (1, 2), \mathbf{e}_2 = (1, 0)$ .

Finally, the point  $P_3$  is an unstable spiral as its eigenvalues  $\lambda_1 = (1 + i\sqrt{7})/2, \lambda_2 = (1 - i\sqrt{7})/2$  are complex conjugate with positive real part, and the eigenvectors are  $\mathbf{e}_1 = (2\lambda_1, 1)$  and  $\mathbf{e}_2 = (2\lambda_2, 1)$ . Therefore

$$\begin{pmatrix} \delta x(t) \\ \delta y(t) \end{pmatrix} = c_1 \begin{pmatrix} 1 \\ 2 \end{pmatrix} \exp(-t) + c_2 \begin{pmatrix} 1 \\ 0 \end{pmatrix} \exp(t) .$$

Having identified the behavior of trajectories around the fixed points it is now rather easy to sketch the qualitative behavior in phase space which looks like in Fig.2.

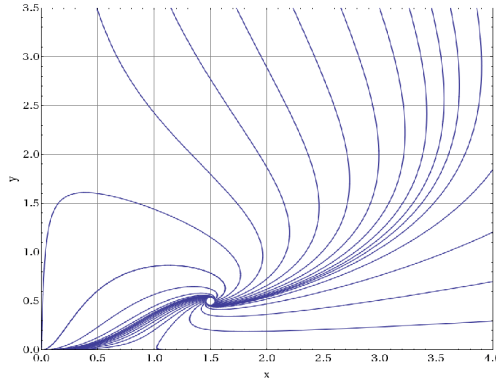
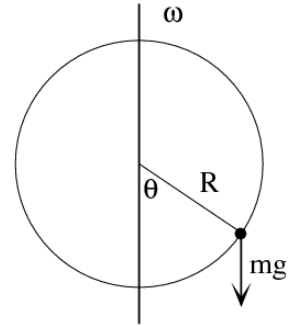


FIG. 2: Trajectory behaviours around the saddle fixed point  $P_3$ .

### Exercise 2.6

A rigid hoop of radius  $R$  hangs from the ceiling and a small ring can move without friction along the hoop. The hoop rotates with frequency  $\omega$  about a vertical axis passing through its center as in the figure on the right. Show that if  $\omega < \omega_0 = \sqrt{g/R}$  the bottom of the hoop is a stable fixed point, while if  $\omega > \omega_0$  the stable fixed points are determined by the condition  $\cos \theta^* = g/(R\omega^2)$ .



### Solution

In the rotating frame one has a mechanical system with Kinetic energy  $T = (1/2m)R^2\dot{\theta}^2$  and Potential energy  $V = mgR[1 - \cos \theta] - (1/2m)R^2\omega^2 \sin^2 \theta$  which includes also the centrifugal contribution. The fixed points are given by the condition:

$$\frac{\partial V}{\partial \theta} = mgR \sin \theta - mR^2\omega^2 \sin \theta \cos \theta = 0$$

One solution is  $\theta^* = 0$ , corresponding to the bottom of the hoop. This is the unique solution as long as  $\omega < \sqrt{g/R}$ , in this case since  $\frac{\partial^2 V}{\partial \theta^2}|_{\theta=0} < 0$ , the fixed point is stable (Lagrange theorem).

When  $\omega > \sqrt{g/R}$ ,  $\theta^* = 0$  becomes unstable ( $\frac{\partial^2 V}{\partial \theta^2}|_{\theta=0} > 0$ ) but two other fixed points occur, given by the solution of the equation  $\cos \theta^* = g/(R\omega^2)$ . In Fig.3 we show the shape

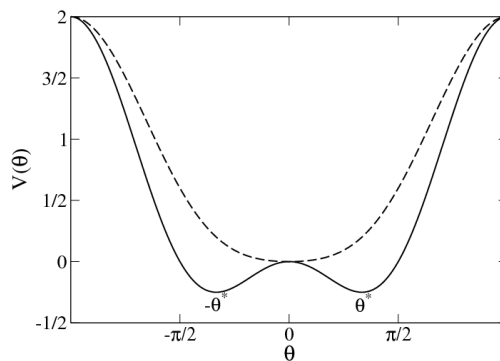


FIG. 3: Potential energy for two values of  $g/(R\omega^2)$  such that  $\omega < \sqrt{g/R}$  (dashed line) and  $\omega > \sqrt{g/R}$  (solid line).



of the potential for two values of  $g/(R\omega^2)$  corresponding to the stability of  $\theta = 0$  (dashed lines) and of the two solutions of  $\cos\theta^* = g/(R\omega^2)$  (solid line).

### Exercise 2.7

Show that the two-dimensional map:

$$x(t+1) = x(t) + f(y(t)), \quad y(t+1) = y(t) + g(x(t+1))$$

is symplectic for any choice of the functions  $g(u)$  and  $f(u)$ .

### Solution

We can start linearizing the map

$$\begin{aligned} \delta x(t+1) &= \delta x(t) + f'(y(t))\delta y(t) \\ \delta y(t+1) &= \delta y(t) + g'(x(t+1))\delta x(t+1) \\ &= \delta y(t) + g'(x(t+1))[\delta x(t) + f'(y(t))\delta y(t)] \end{aligned}$$

from which the stability matrix is easily computed

$$\begin{pmatrix} \delta x(t+1) \\ \delta y(t+1) \end{pmatrix} = \begin{pmatrix} 1 & f'(y(t)) \\ g'(x(t+1)) & 1 + g'(x(t+1))f'(y(t)) \end{pmatrix} \begin{pmatrix} \delta x(t) \\ \delta y(t) \end{pmatrix}.$$

Then we can see that

$$\det \begin{pmatrix} 1 & f'(y(t)) \\ g'(x(t+1)) & 1 + g'(x(t+1))f'(y(t)) \end{pmatrix} = 1 + g'(x(t+1))f'(y(t)) - g'(x(t+1))f'(y(t)) = 1$$

### Exercise 2.8

Show that the one-dimensional non-invertible map

$$x(t+1) = \begin{cases} 2x(t) & x(t) \in [0:1/2]; \\ c & x(t) \in [1/2:1] \end{cases}$$

with  $c < 1/2$ , admits superstable periodic orbits, i.e. after a finite time the trajectory becomes periodic.

### Solution

First of all to have a qualitative idea of the map, in Fig.4 we plot it for  $c < 0.3$ .

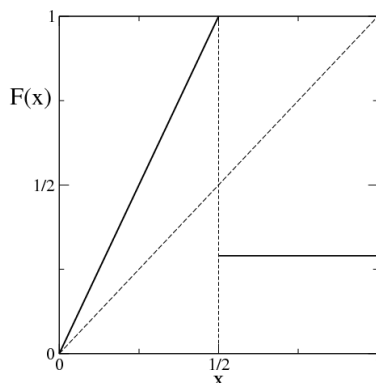


FIG. 4: Plot of the map for  $c = 0.3$

Consider now two classes of initial conditions: a)  $x(0) \in [1/2:1]$  and b)  $x(0) \in [0:1/2]$ .

If the initial condition belong to class a), the first iterate of the map is  $x(1) = c$ , then  $x(t)$  will be smaller than  $1/2$  for  $t < t_*$ , where  $t_*$  is determined by the conditions  $x(t_* - 1) = 2^{t_*-2}c < 1/2$ ,  $2^{t_*-2}c \geq 1/2$ . Therefore,  $x(t_*)$  will be in the set  $[1/2 : 1]$  and accordingly  $x(t_* + 1) = c = x_1$ , i.e. the orbit is periodic.

In the case b), for all initial conditions  $x(1) \in [1/2:1]$ , so that the reasoning of the case a) can be repeated.

### Exercise 2.9

*Discuss the qualitative behavior of the system*

$$\frac{dx}{dt} = xg(y), \quad \frac{dy}{dt} = -yf(x)$$

*under the conditions that  $f(x)$  and  $g(x)$  are differentiable decreasing functions such that  $f(0) > 0, g(0) > 0$ , moreover there is a point  $(x^*, y^*)$ , with  $x^*, y^* > 0$ , such that  $g(x^*) = f(y^*) = 0$ . Compare the dynamical behavior of the system with that of the Lotka-Volterra model (Sec. 11.3.1).*

### Solution

The fixed points of the system are:  $P_1 = (0, 0)$  and  $P_2 = (x^*, y^*)$ .  $P_1$  is an hyperbolic point, indeed its stability matrix is

$$\mathbb{L}_0 = \begin{pmatrix} g(0) & 0 \\ 0 & -f(0) \end{pmatrix}$$

with eigenvalues  $\lambda_1 = g(0) > 0$  and  $\lambda_2 = -f(0) < 0$ .

While the stability of  $P_2$  is characterized by the matrix

$$\mathbb{L}_1 = \begin{pmatrix} 0 & x^* g'(y^*) \\ -y^* f'(x^*) & 0 \end{pmatrix}.$$

whose eigenvalues are imaginary  $\lambda_{1,2} = \pm \sqrt{x^* y^* f'(x^*) g'(y^*)}$  as the functions  $f$  and  $g$  are decreasing (i.e.  $f' < 0$  and  $g' < 0$ ).

Noting that if  $x$  and  $y$  are positive they cannot change their sign one can introduce the variables  $p = \ln(x)$  and  $q = \ln(y)$ .

$$\begin{aligned} \frac{dq}{dt} &= g(e^p) = \frac{\partial H}{\partial p} \\ \frac{dp}{dt} &= -f(e^q) = -\frac{\partial H}{\partial q} \end{aligned}$$

the system has an Hamiltonian structure with

$$H(p, q) = \int_{p_0}^p du g(e^u) + \int_{q_0}^q du f(e^u)$$

Since the system is autonomous and Hamiltonian  $H = \text{const}$ , the trajectories evolve along the isolines of  $H$ , therefore the motion is periodic.

Notice that the Lotka-Volterra equations:

$$\begin{aligned} \frac{dx}{dt} &= r_1 x - \gamma_1 x y = x(r_1 - \gamma_1 y) \\ \frac{dy}{dt} &= -r_2 y + \gamma_2 x y = -y(r_2 - \gamma_2 x) \end{aligned}$$

correspond to a subclass of the analyzed model, in which the function  $g$  and  $f$  are linear.

### Exercise 2.10

Consider the autonomous system

$$\frac{dx}{dt} = yz, \quad \frac{dy}{dt} = -2xz, \quad \frac{dz}{dt} = xy$$

1. show that  $x^2 + y^2 + z^2 = \text{const}$ ;
2. discuss the stability of the fixed points, inferring the qualitative behavior on the sphere defined by  $x^2 + y^2 + z^2 = 1$ ;
3. Discuss the generalization of the above system:

$$\frac{dx}{dt} = ayz, \quad \frac{dy}{dt} = bxz, \quad \frac{dz}{dt} = cxy$$

where  $a, b, c$  are non-zero constants with the constraint  $a + b + c = 0$ .

### Solution

- 1) Deriving  $x^2 + y^2 + z^2$  with respect to time and using the equation of motion it is easily obtained the conservation of the quantity.
- 1) On the unitary sphere  $S: x^2 + y^2 + z^2 = 1$  we have six fixed points:  $(\pm 1, 0, 0)$ ,  $(0, \pm 1, 0)$ ,  $(0, 0, \pm 1)$ . The stability matrix of the system is:

$$\mathbb{L} = \begin{pmatrix} 0 & z & y \\ -2z & 0 & -2x \\ y & x & 0 \end{pmatrix}.$$

An easy computation shows that the six fixed points are characterized by the following eigenvalues

$(\pm 1, 0, 0)$   $\lambda_1 = 0$  and  $\lambda_{2,3} = \pm i\sqrt{2}$  so that the point is a center;

$(0, \pm 1, 0)$   $\lambda_1 = 0$  and  $\lambda_{2,3} = \pm 1$  so that the point is a saddle;

$(0, 0, \pm 1)$   $\lambda_1 = 0$  and  $\lambda_{2,3} = \pm i\sqrt{2}$  so that the point is a center;

Computing the eigendirection associated to  $\lambda_1 = 0$  one can convince himself/herself that the marginal direction is always associated to the direction perpendicular to the sphere, thanks to the conservation law. As usual when a linear stability analysis is performed we cannot be completely sure that nonlinear terms will not modify the stability properties of the fixed point. As discussed in Sec.2.4.2, this is particular relevant to marginal cases such as when the point is a center. In the examined example, we can overcome such a difficulty noticing that there are other three conservation laws namely

$$I_1 = x^2 + \frac{y^2}{2} = \text{const}, \quad I_2 = \frac{y^2}{2} + z^2 = \text{const}, \quad I_3 = x^2 - z^2 = \text{const}.$$

As a consequence, the trajectories should evolve along the intersections between the unitary sphere and the surfaces identified by the previous equations. In particular, the surfaces  $I_1$  and  $I_2$  are cylinders centered at the origin and perpendicular to the planes  $x, y$  and  $y, z$ , respectively these cylinders intersect the sphere along ellipses implying that  $(0, 0, \pm 1)$  and  $(\pm 1, 0, 0)$  are centers, thus confirming the linear stability result. On the other hand  $I_3$  is a hyperboloid whose intersection with the unitary sphere confirms that  $(0, \pm 1, 0)$  are saddles. Fig.5 shows the trajectories originating from the system on the unitary sphere.

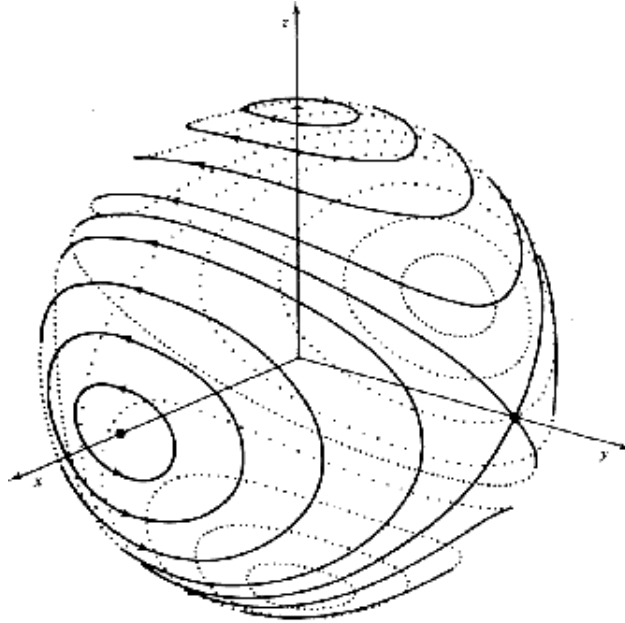


FIG. 5: Trajectories evolving along the intersections between  $I_1 = \text{const}$  and  $x^2 + y^2 + z^2 = 1$ .

c) Consider the case  $(a, c) > 0$  and  $b < 0$  (the remaining cases can be obtained with obvious changes). One has:  $x^2 + y^2 + z^2 = \text{const}$  and the additional constants of motion are

$$\frac{x^2}{a} + \frac{y^2}{|b|} = \text{const} \quad (1)$$

$$\frac{z^2}{c} + \frac{y^2}{|b|} = \text{const} \quad (2)$$

$$\frac{x^2}{a} - \frac{y^2}{c} = \text{const} . \quad (3)$$

It is not difficult to realize that the previous arguments apply also to this case.

## CHAPTER 3: Examples of Chaotic Behaviours

### Exercise 3.1

Study the stability of the map  $f(x) = 1 - ax^2$  at varying  $a$  with  $x \in [-1 : 1]$ , and numerically compute its bifurcation tree using the method described for the logistic map.

### Solution

Intuition should suggest that with a linear change of variables we should be able to reduce the map  $x(t+1) = 1 - ax(t)^2$  to the standard form of the logistic map. Choose the general linear transformation  $x(t) = \alpha + \beta y(t)$ , and we need to find  $\alpha, \beta$  such that  $y(t+1) = Ay(t)(1 - y(t))$ . A direct substitution in the map  $x(t+1) = 1 - ax(t)^2$  provides the expression

$$\alpha + \beta y(t+1) = 1 - a[\alpha + \beta y(t)]^2$$

expanding and rearranging, we arrive at

$$y(t+1) = \frac{1 - \alpha - a\alpha^2}{\beta} - 2a\alpha \left[ y(t) + \frac{\beta}{2\alpha} y(t)^2 \right]$$

Now imposing that  $1 - \alpha - a\alpha^2 = 0$  and  $\beta = -2\alpha$ , we obtain the standard form

$$y(t+1) = Ay(t)(1 - y(t))$$

with  $A = \sqrt{1 + 4a} - 1$  as  $\alpha = \sqrt{1 + 4a}/2a - 1$  (the negative solution  $\alpha = -\sqrt{1 + 4a}/2a - 1$  is not acceptable because  $A$  must be positive). Note that the final transformation results  $x(t) = \alpha(1 - 2y(t))$  with only a free parameter. Of course, once the bifurcation tree of the logistic map is known the solution of the exercises is simply obtained by changing the variables. Notice that this changes of variable leave the basic shape of the bifurcation tree unchanged.

### Exercise 3.2

Consider the logistic map for  $r^* = 1 + \sqrt{8}$ . Study the bifurcation diagram for  $r > r^*$ , which kind of bifurcation do you observe? What does happen at the trajectories of the logistic map for  $r \leq r^*$  (e.g.  $r = r^* - \epsilon$ , with  $\epsilon = 10^{-3}, 10^{-4}, 10^{-5}$ )? (If you find it curious look at the second question of Ex.3.4 and then at Ex.6.4).

### Hints and Solution

At  $r^* = 1 + \sqrt{8}$  the logistic map has a period-3 orbit, for  $r < r^*$  is chaotic, but a special kind of chaos as you can recognize plotting a generic trajectory. A trick to understand the origin of this regime is to plot the third iterate of the map and look close to the region close to  $x = 1/2$ : what does happen at reducing  $r$  from  $r^*$  (compare it with what does happen in Fig.6.6 Chapter.6). The bifurcation tree above  $r > r^*$  shows a period doubling transition to chaos but starting from an orbit of period-3. Consequently, we have a period doubling to orbits of period 6,12,... See Ex.6.4 for more insights.

### Exercise 3.3

*Numerically study the bifurcation diagram of the sin map*

$$x(t + 1) = r \sin(\pi x(t))$$

*for  $r \in [0.6:1]$ , is it similar to the one of the logistic map?*

### Hints and Solution

Performing the simulation you will realize a perfect similarity with the bifurcation tree of the logistic map. Trying with any other map with a quadratic maximum in the middle of the unit interval and you will obtain similar bifurcation trees. This is not a simple circumstance but the evidence of some “universal” behavior, whose roots are explained in Sec. 6.2 and 6.2.1.

### Exercise 3.4

*Study the behavior of the trajectories (attractor shape, time series of  $x(t)$  or  $z(t)$ ) of the Lorenz system with  $\sigma = 10$ ,  $b = 8/3$  and let  $r$  vary in the regions:*

1.  $r \in [145:166]$ ;
2.  $r \in [166:166.5]$  (after compare with the behavior of the logistic map seen in Ex.);
3.  $r \approx 212$ ;



### Hints and Solution

Integrate numerically the Lorenz system via a 4th-order Runge-Kutta algorithm which can be found in many manuals of algorithms, as e.g. Numerical Recipes. As for  $r \approx 166$  compare with the results presented in Sec. 6.3.

#### Exercise 3.5

*Draw the attractor of the Rössler system*

$$\begin{aligned}\frac{dx}{dt} &= -y - z, \\ \frac{dy}{dt} &= x + ay \\ \frac{dz}{dt} &= b + z(x - c)\end{aligned}$$

for  $a=0.15$ ,  $b=0.4$  and  $c=8.5$ . Check that also for this strange attractor there is sensitivity to initial conditions.

### Hints and Solution

For comparison you can take a look to Fig.11.19 in Ch.11.

#### Exercise 3.6

*Consider the two-dimensional map*

$$x(t+1) = 1 - a|x(t)|^m + y(t), \quad y(t+1) = bx(t)$$

for  $m = 1$  and  $m = 2$  it reproduces the Hénon and Lozi map, respectively. Determine numerically the attractor generated with  $(a = 1.4, b = 0.3)$  in the two cases. In particular, consider an ensemble initial conditions  $(x^{(k)}(0), y^{(k)}(0))$ , ( $k = 1, \dots, N$  with  $N = 10^4$  or  $N = 10^5$ ) uniformly distributed on a circle of radius  $r = 10^{-2}$  centered in the point  $(x_c, y_c) = (0, 0)$ . Plot the iterates of this ensemble of points at times  $t = 1, 2, 3, \dots$  and observe the relaxation onto the Hénon (Fig. 5.1) and Lozi attractors.

### Hints and Solution

The Lozi attractor should look as in Fig.6

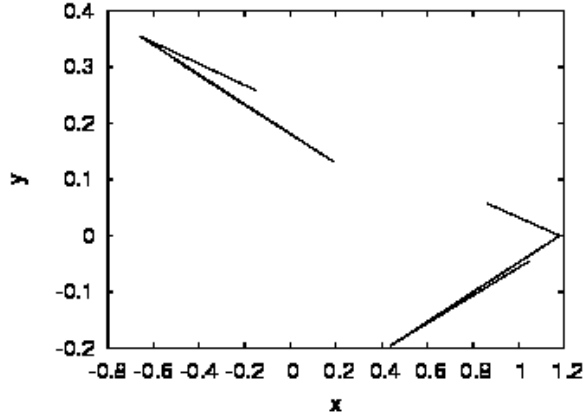


FIG. 6: Lozi attractor.

### Exercise 3.7

Consider the following two-dimensional map

$$x(t+1) = y(t), \quad y(t+1) = -bx(t) + dy(t) - y^3(t).$$

Display the different attractors in a plot  $y(t)$  vs  $d$ , obtained by setting  $b = 0.2$  and varying  $d \in [2.0 : 2.8]$ . Discuss the bifurcation diagram. In particular, examine the attractor at  $d = 2.71$ .

### Exercise 3.8

Write a computer code to reproduce the Poincaré sections of the Hénon-Heiles system shown in Fig. 4.5.

### Exercise 3.9

Consider the two-dimensional map [Hénon-Heiles (1964)]

$$x(t+1) = x(t) + a(y(t) - y^3(t)), \quad y(t+1) = y(t) - a(x(t+1) - x^3(t+1))$$

show that it is symplectic and numerically study the behavior of the map for  $a = 1.6$  choosing a set of initial conditions in  $(x, y) \in [-1 : 1] \times [-1 : 1]$ . Does the phase-portrait look similar to the Poincaré section of the Hénon-Heiles system?

## Hints and Solution

Use the results of the Exercise 2.7. The phase portrait can be found in the original work by Hénon and Helies. Pay attention to the fact that chaotic orbits can rapidly escape to infinity due to the cubic terms, therefore in the plot one has to constraint the number of iterations.

### Exercise 3.10

Consider the forced van der Pol oscillator

$$\frac{dx}{dt} = y, \quad \frac{dy}{dt} = -x + \mu(1-x)y + A \cos(\omega_1 t) \cos(\omega_2 t)$$

Set  $\mu = 5.0$ ,  $F = 5.0$ ,  $\omega_1 = \sqrt{2} + 1.05$ . Determine numerically the asymptotic evolution of the system for  $\omega_2 = 0.002$  and  $\omega_2 = 0.0006$ . Discuss the features of the two attractors by using a Poincaré section.

**Hint:** Integrate numerically the system via a Runge-Kutta algorithm

### Exercise 3.11

Given the dynamical laws  $x(t) = x_0 + x_1 \cos(\omega_1 t) + x_2 \cos(\omega_2 t)$ , compute its auto-correlation function:

$$C(\tau) = \langle x(t)x(t+\tau) \rangle = \lim_{T \rightarrow \infty} \frac{1}{T} \int_0^T dt x(t)x(t+\tau).$$

## Solution

Using the trigonometric identity  $\cos(\alpha) \cos(\beta) = 1/2[\cos(\alpha + \beta) + \cos(\alpha - \beta)]$  and noting that

$$\lim_{T \rightarrow \infty} \frac{1}{T} \int_0^T dt \cos(\omega t) = 0$$

it is easy to compute

$$C(\tau) = x_0^2 + \frac{1}{2} \left[ x_1^2 \cos(\omega_1 \tau) + x_2^2 \cos(\omega_2 \tau) \right]$$

**Exercise 3.12**

Numerically compute the correlation function  $C(t) = \langle x(t)x(0) \rangle - \langle x(t) \rangle^2$  for:

1. Hénon map (see Ex.) with  $a = 1.4, b = 0.3$ ;
2. Lozi map (see Ex.) with  $a = 1.4, b = 0.3$ ;
3. Standard map (see Eq. (2.18)) with  $K = 8$ , for a trajectory starting from the chaotic sea.

## CHAPTER 4: Probabilistic Approach to Chaos

### Exercise 4.1

Numerically study the time evolution of  $\rho_t(x)$  for the logistic map  $x(t+1) = r x(t) (1 - x(t))$  with  $r = 4$ . Use as initial condition

$$\rho_0(x) = \begin{cases} 1/\Delta & \text{if } x \in [x_0 : x_0 + \Delta] \\ 0 & \text{elsewhere} \end{cases},$$

with  $\Delta = 10^{-2}$  and  $x_0 = 0.1$  or  $x_0 = 0.45$ . Look at the evolution and compare with the invariant density  $\rho^{inv}(x) = (\pi\sqrt{x(1-x)})^{-1}$ .

### Exercise 4.2

Consider the map  $x(t+1) = x(t) + \omega \pmod{1}$  and show that

- (1) the Lebesgue measure in  $[0:1]$  is invariant;
- (2) the map is periodic if  $\omega$  is rational;
- (3) the map is ergodic if  $\omega$  is irrational.

### Solution

In order to prove statement

- 1) it is enough to note that  $\delta x(t+1) = \delta x(t)$  (conservation of volumes).
- 2) If  $\omega$  is rational, there are two integers  $p$  and  $q$  such that  $\omega = p/q$ . The trajectory of the system  $x(t+1) = x(t) + \omega \pmod{1}$ , stemming from the initial condition  $x_0$ , is given by

$$x(t) = x_0 + \omega t \pmod{1} = x_0 + (p/q)t \pmod{1} \quad (4)$$

therefore for  $t = kq$  the motion returns to  $x_0$ , and thus is periodic of period  $q$ .

- 3) To prove the statement, it is convenient to consider the smooth function in the interval  $[0:1]$  which we can express in terms of Fourier series

$$A(x) = A_0 + \sum_{n \neq 0}^{\infty} A_n \exp(2\pi i n x)$$

where  $A_0 = \int_0^1 dx A(x)$  is the phase average. The solution  $x(t) = x_0 + \omega t \pmod{1}$  implies

that the time average is computed as:

$$\overline{A(x)}^T = \frac{1}{T} \sum_0^{T-1} A(x(t)) = A_0 + \frac{1}{T} \sum_0^{T-1} \sum_{n \neq 0}^{\infty} A_n \exp\{2\pi i n(x_0 + \omega t)\}$$

that, recalling geometric-series summation formula, becomes

$$\overline{A(x)}^T = A_0 + \sum_{n \neq 0}^{\infty} A_n \exp(2\pi i n x_0) \frac{1}{T} \left[ \frac{1 - e^{2\pi i n \omega T}}{1 - e^{2\pi i n \omega}} \right]$$

If  $\omega$  is irrational  $n\omega$  cannot be an integer, thus  $|\exp(2\pi i n \omega)| < 1$  the limit  $T \rightarrow \infty$  implies that  $\overline{A(x)}^T \rightarrow A_0$ , that is the time average coincides with the phase average.

### Exercise 4.3

Consider the two-state Markov Chain defined by the transition matrix

$$\mathbb{W} = \begin{pmatrix} p & 1-p \\ 1-p & p \end{pmatrix} :$$

provide a graphical representation; find the invariant probabilities; show that a generic initial probability relax to the invariant one as  $\mathbf{P}(t) \approx \mathbf{P}^{inv} + \mathcal{O}(e^{-t/\tau})$  and determine  $\tau$ ; explicitly compute the correlation function  $C(t) = \langle x(t)x(0) \rangle$  with  $x(t) = 1, 0$  if the process is in the state 0 or 1.

### Solution

A simple graphical representation of this Markov chain is as in Fig.7.

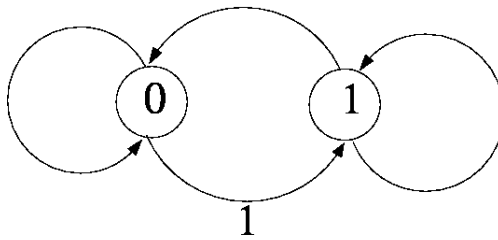


FIG. 7: Graphical representation of the Markov chain.

Indicate with  $P(t) = P_0(t)$  the probability to have the state 1 at time  $t$ , accordingly  $P_1(t) = 1 - P_0(t) = 1 - P(t)$ , therefore we can write the evolution equation as

$$P(t+1) = pP(t) + (1-p)[1 - P(t)] = (1-p) + (2p-1)P(t) \quad (5)$$

whose solution is

$$P(t) = \frac{1}{2} + (2p - 1)^t \left( P(0) - \frac{1}{2} \right) \xrightarrow{t \rightarrow \infty} P_0^{inv} = \frac{1}{2}.$$

For the variable  $\delta P(t) = P(t) - 1/2$ , the above equation becomes  $\delta P(t) = (2p - 1)^t \delta P(0)$  and it turns clear that the convergence is controlled by the time  $\tau = -1/\ln |2p - 1|$ .

We can write  $\langle x(t)x(0) \rangle$  as  $\langle \chi_0(t)\chi_0(0) \rangle$  where  $\chi_0(t) = 1$  if the system occupies the state 0, otherwise  $\chi_0(t) = 0$ . From the discussion in Box.B6 we have

$$\langle x(t)x(0) \rangle = P_1^{inv} W_{00}^t$$

where  $W_{00}^t$  is nothing but  $P(t) = 1/2 + 1/2(2p - 1)^t$ , i.e. the solution of (5) with  $P(0) = 1$  then

$$\langle x(t)x(0) \rangle = \frac{1}{4} + \frac{1}{4}(2p - 1)^t.$$

#### Exercise 4.4

*Consider the Markov Chains defined by the transition probabilities*

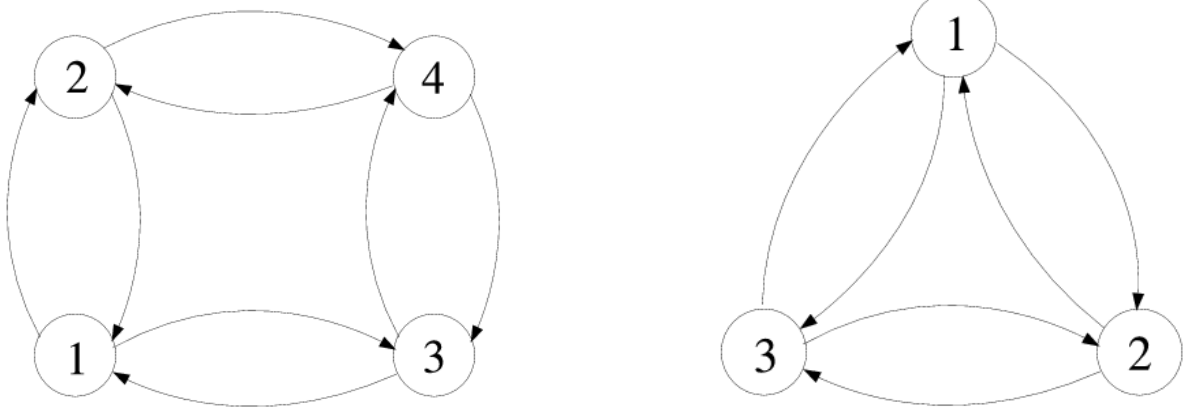
$$\mathbb{F} = \begin{pmatrix} 0 & 1/2 & 1/2 & 0 \\ 1/2 & 0 & 0 & 1/2 \\ 1/2 & 0 & 0 & 1/2 \\ 0 & 1/2 & 1/2 & 0 \end{pmatrix} \quad \mathbb{T} = \begin{pmatrix} 0 & 1/2 & 1/2 \\ 1/2 & 0 & 1/2 \\ 1/2 & 1/2 & 0 \end{pmatrix}$$

*which describe a random walk within a ring of 4 and 3 states, respectively.*

- (1) provide a graphical representation of the two Markov Chains;*
- (2) find the invariant probabilities in both cases;*
- (3) is the invariant probability asymptotically reached from any initial condition?*
- (4) after a long time what is the probability of visiting each state?*
- (5) generalize the problem to the case with  $2n$  or  $2n + 1$  states, respectively.*

#### Solution

- 1) The graphs associated to the Markov Chains  $F$  and  $T$  are respectively
- 2) Observe that matrices  $\mathbb{T}$  and  $\mathbb{F}$  are such that summation along each row and each column gives 1 (when this condition is satisfied the matrix is said to be doubly stochastic),



$\sum_i \mathbb{T}_{ij} = \sum_j \mathbb{T}_{ij} = 1$  and  $\sum_i \mathbb{F}_{ij} = \sum_j \mathbb{F}_{ij} = 1$ . This property implies that they admit a constant invariant density i.e. the eigenvector with eigenvalue 1 has constant entries  $p_i = a$  ( $i = 1, \dots, 4$ ) this can be easily verified as

$$a = p_i = \sum_j \mathbb{T}_{ij} p_j = a \sum_j \mathbb{T}_{ij} = a.$$

Therefore, the invariant distributions for  $\mathbb{T}$  and  $\mathbb{F}$  are  $P^{inv} = (1/3, 1/3, 1/3)$  and  $P^{inv} = (1/4, 1/4, 1/4, 1/4)$ , respectively.

3) The Markov Chain  $\mathbb{T}$  is ergodic, this can be proved showing that  $\mathbb{T}^n$  tend to a matrix composed by the invariant probability. As an alternative, equivalent (the algebra is the same), method here we consider a specific initial condition, namely  $P(t = 0) = (1, 0, 0)$ , and show that  $P(t \rightarrow \infty) \rightarrow (1/3, 1/3, 1/3)$ . A straightforward implementation of the evolution rule for the probabilities show that if  $P(t = 0) = (1, 0, 0)$  then  $P(t = 1) = (0, 1/2, 1/2)$ ,  $P(t = 2) = (1/2, 1/4, 1/4)$ , generically for  $k \geq 1$  we can write  $P(t = k) = [F(k-2)/2^{k-1}, F(k-1)/2^k, F(k-1)/2^k]$  with  $F(k)$  given by the recursion  $F(k) = F(k-1) + 2F(k-2)$  with initial conditions  $F(-1) = 0$  and  $F(0) = 1$ . Now we need to understand the asymptotic behavior of the term  $F(k)/2^{k+1}$ , to do so it is necessary to solve the recursion:

$$F(k) = F(k-1) + 2F(k-2) \quad F(-1) = 0, F(0) = 1$$

the standard method assume an asymptotic solution of the form  $F(k) = \lambda^k$  which plugged in the recursion means to solve the quadratic equation

$$\lambda^2 - \lambda - 2 = 0$$



whose solutions are  $\lambda_1 = -1$  and  $\lambda_2 = 2$ . The solution will thus be of the form

$$F(k) = A\lambda_1^k + B\lambda_2^k$$

where  $A$  and  $B$  are determined by the initial conditions, thus to finalize the solution we simply need to solve the linear system:

$$-A + B/2 = 0 \quad A + B = 1$$

which means  $A = 1/3$  and  $B = 2/3$ , therefore we have

$$\frac{F(k)}{2^{k+1}} = \frac{\frac{(-1)^k}{3} + \frac{2^{k+1}}{3}}{2^{k+1}} \rightarrow \frac{1}{3}$$

proving the asymptotic convergence to the invariant distribution. One can easily convince himself/herself that such a property holds for generic initial conditions.

A visual reasoning on the graph of the Markov Chain defined by matrix  $\mathbb{F}$  should convince the reader that the MC is periodic indeed as  $P(t = 0) = (1, 0, 0, 0) \rightarrow P(t = 1) = (0, 1/2, 1/2, 0) \rightarrow P(t = 2) = (1/2, 0, 0, 1/2) \rightarrow P(t = 3) = (0, 1/2, 1/2, 0) = P(t = 1)$ .

4) As the Markov Chain  $\mathbb{F}$  relaxes to the invariant distribution the probability of visiting a certain state is  $1/3$ . For the Markov Chain  $\mathbb{F}$  such a probability is  $1/4$ , on average. But, more precisely, this is realized in a different way, for example: if  $P(t = 0) = (1, 0, 0, 0)$  at time  $t = 2k$ , the probability to visit states 1 and 4 is  $1/2$ , while for states 2 and 3 this probability is 0. Viceversa, at time  $t = 2k + 1$ , the probability is 0 to visit states 1 and 4, while states 2 and 3 are visited with probability is  $1/2$  each.

5) It is easy to realize (for instance, considering the initial condition  $P(t = 0) = (1, 0, \dots, 0)$ ) that the odd  $(2n + 1)$  and even  $(2n)$  number of states are similar to the three and four state cases, respectively.

### Exercise 4.5

*Consider the standard map*

$$I(t + 1) = I(t) + K \sin(\phi(t)) \pmod{2\pi}, \quad \phi(t + 1) = \phi(t) + I(t + 1) \pmod{2\pi},$$

*and numerically compute the pdf of the time return function in the set  $A = \{(\phi, I) : (\phi - \phi_0)^2 + (I - I_0)^2 < 10^{-2}\}$  for  $K = 10$ , with  $(\phi_0, I_0) = (1.0, 1.0)$  and  $K = 0.9$ , with  $(\phi_0, I_0) = (0, 0)$ . Compare the results with the expectation for ergodic systems (Box B.7).*

### Exercise 4.6

Consider the Gauss map defined in the interval  $[0:1]$  by  $F(x) = x^{-1} - [x^{-1}]$  if  $x \neq 0$  and  $F(x=0) = 0$ , where  $[...]$  denotes the integer part. Verify that  $\rho(x) = \frac{1}{\ln 2} \frac{1}{1+x}$  is an invariant measure for the map.

### Solution

This exercise is an application of the Perron-Frobenius operator. The invariant measure  $\rho(x) = \frac{C}{1+x}$  ( $C = 1/\ln 2$ ) should satisfy the identity

$$\rho(x) = \sum_{n=1}^{\infty} \frac{\rho(y_n)}{|F'(y_n)|} = \sum_{n=1}^{\infty} \frac{C}{|F'(y_n)|(1+y_n)} \quad (6)$$

where  $y_n$  are the pre-images of  $x$ :  $F(y_n) = x$  which by definition are given by

$$\frac{1}{y_n} - n = x \longrightarrow y_n = \frac{1}{x+n}$$

with  $n = 1, 2, 3, \dots$  and  $|F'(y_n)| = y_n^{-2} = (x+n)^2$ , therefore Eq.(6) becomes

$$\frac{1}{1+x} = \sum_{n=1}^{\infty} \frac{1}{x+n} \cdot \frac{1}{x+n+1}.$$

via the identity

$$\frac{1}{x+n} \cdot \frac{1}{x+n+1} = \frac{1}{x+n} - \frac{1}{x+n+1}$$

we can write the r.h.s member as

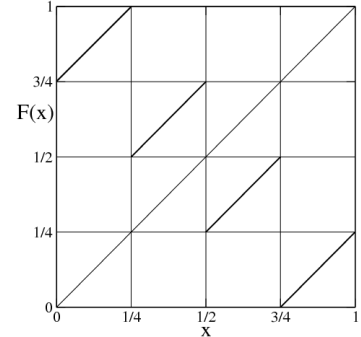
$$\sum_{n=1}^{\infty} \left( \frac{1}{x+n} - \frac{1}{x+n+1} \right) = \frac{1}{1+x} - \frac{1}{2+x} + \frac{1}{2+x} - \frac{1}{3+x} + \frac{1}{3+x} + \dots$$

only the term  $1/(1+x)$  survives the perfect cancellation which proves that  $C/(1+x)$  is the invariant measure.

**Exercise 4.7**

Show that the one-dimensional map defined by the equation (see figure on the right)

$$x(t+1) = \begin{cases} x(t) + 3/4 & 0 \leq x(t) < 1/4 \\ x(t) + 1/4 & 1/4 \leq x(t) < 1/2 \\ x(t) - 1/4 & 1/2 \leq x(t) < 3/4 \\ x(t) - 3/4 & 3/4 \leq x(t) \leq 1 \end{cases}$$



is not ergodic with respect to the Lebesgue measure which is invariant.

**Solution**

Because of the first Birkhoff's theorem on ergodicity, to prove the statement of the exercise, it is sufficient to show that there exist two disjoint invariant sets whose measure is neither 0 nor 1. Let us note that the sets  $I_1 = [1/4 : 3/4]$  and  $I_2 = [0 : 1/4] \cup [3/4 : 1]$  have both measure  $1/2$  and are invariant under the map.

**Exercise 4.8**

Numerically investigate the Arnold cat map and reproduce Fig.4.5, compute also the auto-correlation function of  $x$  and  $y$ .

**Exercise 4.9**

Consider the map defined by  $F(x) = 3x \pmod 1$  and show that the Lebesgue measure is invariant. Then consider the characteristic function  $\chi(x) = 1$  if  $x \in [0 : 1/2]$  and zero elsewhere. Numerically verify the ergodicity of the system for a set of generic initial conditions, in particular study how the time average  $1/T \sum_{t=0}^T \chi(x(t))$  converges to the expected value  $1/2$  for generic initial conditions and, in particular for  $x(0) = 7/8$ , what's special in this point? Compute also the correlation function  $\langle \chi(x(t+\tau))\chi(x(t)) \rangle - \langle \chi(x(t)) \rangle^2$  for generic initial conditions.

## Solution

The graph of the map is shown in Fig.8, clearly repeating the construction used in Fig.4.3 in Chapter 4 one can write the PF equation as

$$\rho_{t+1}(x) = \frac{1}{3}\rho_t\left(\frac{x}{3}\right) + \frac{1}{3}\rho_t\left(\frac{x}{3} + \frac{1}{3}\right) + \frac{1}{3}\rho_t\left(\frac{x}{3} + \frac{2}{3}\right) ,$$

which is solved by the uniform distribution of the unit interval  $\rho(x) = 1$ .

Similarly to the Bernoulli map, this generalization admits unstable periodic orbits for rationals, one can understand it using the base 3 representation of numbers. Notice that  $x = 7/8$  lies on a period 2 orbit, so that in this case the temporal average of the characteristic function is 0, indeed one has  $x(2n) = 7/8$  and  $x(2n + 1) = 5/8$  which are both above  $1/2$ .

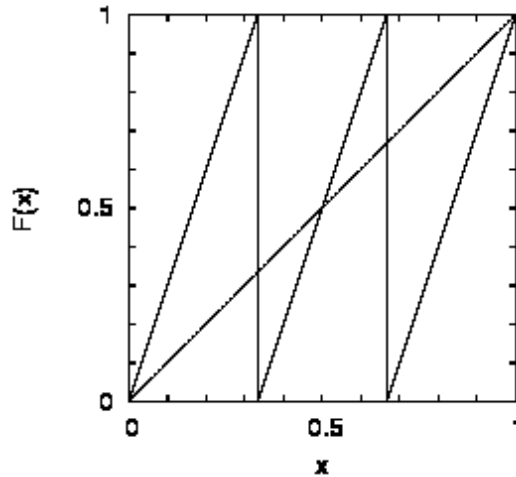


FIG. 8: Graph of the map  $F(x) = 3x$ .

**Exercise 4.10**

Consider the roof map defined by

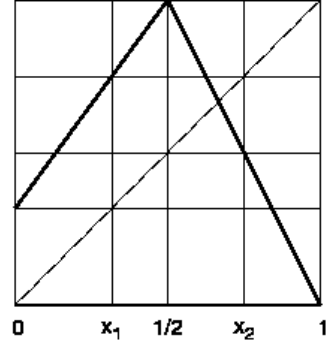
$$F(x) = \begin{cases} F_l(x) = a + 2(1-a)x & 0 \leq x < 1/2 \\ F_r(x) = 2(1-x) & 1/2 \leq x < 1 \end{cases}$$

with  $a = (3 - \sqrt{3})/4$ . Consider the points  $x_1 = F_l^{-1}(x_2)$  and  $x_2 = F_r^{-1}(1/2) = 3/4$  where  $F_{l,r}^{-1}$  is the inverse of the  $F_{l,r}$  map show that

(1)  $[0 : 1/2[ \quad ]1/2 : 1]$  is not a Markov partition;

(2)  $[0 : x_1[ \quad ]x_1 : 1/2[ \quad ]1/2 : x_2[ \quad ]x_2 : 1]$  is a Markov partition and compute the transition matrix;

(3) compute the invariant density.



**Solution**

- 1) The intervals of the partition  $[0 : 1/2[$ ,  $]1/2 : 1]$  are such that:  $F(0) = a = (3 - \sqrt{3})/4 \neq 1/2$ , this is sufficient to say that the partition is not a Markov partition.
- 2) The intervals of the partition  $[0 : x_1[$ ,  $]x_1 : 1/2[$ ,  $]1/2 : x_2[$ ,  $]x_2 : 1]$  (with  $x_1 = a$  and  $x_2 = 3/4$ ) are such that  $F(0) = x_1$ ,  $F(x_1) = x_2$ ,  $F(x_2) = 1/2$ ,  $F(1) = 0$ , therefore the partition is Markov.
- 3) Indicating with  $\rho_1^{inv}, \dots, \rho_4^{inv}$  the value of invariant measure the sets  $[0 : x_1[$ ,  $]x_1 : 1/2[$ ,  $]1/2 : x_2[$ ,  $]x_2 : 1]$  respectively, we have

$$\begin{aligned} \rho_1^{inv} &= \frac{1}{2} \rho_4^{inv} \\ \rho_2^{inv} &= \frac{1}{2(1-a)} \rho_1^{inv} + \frac{1}{2} \rho_4^{inv} \\ \rho_3^{inv} &= \frac{1}{2(1-a)} \rho_1^{inv} + \frac{1}{2} \rho_3^{inv} \\ \rho_4^{inv} &= \frac{1}{2(1-a)} \rho_2^{inv} + \frac{1}{2} \rho_3^{inv} . \end{aligned}$$

the above linear equations in matrix form read  $\rho^{inv} = \mathbb{A}\rho^{inv}$ , where (recalling the value of  $a$ )

$$\mathbb{A} = \begin{pmatrix} 0 & 0 & 0 & 1/2 \\ \sqrt{3}-1 & 0 & 0 & 1/2 \\ \sqrt{3}-1 & 0 & 1/2 & 0 \\ 0 & \sqrt{3}-1 & 1/2 & 0 \end{pmatrix}.$$

The eigenvector of  $\mathbb{A}$ ,  $\mathbf{Q}^* = (1/2, \sqrt{3}/2, \sqrt{3}-1, 1)$ , with eigenvalue 1, determines the stationary distribution upon the normalization  $\rho^{inv} = C\mathbf{Q}^*$ ,

$$C \left( Q_1^* \frac{3-\sqrt{3}}{4} + Q_2^* \frac{\sqrt{3}-1}{4} + Q_3^* \frac{1}{4} + Q_4^* \frac{1}{4} \right) = 1$$

this defines the normalization constant  $C = 3/4$ . Then the final distribution is

$$\rho^{inv} = \left( \frac{2}{3}, \frac{2}{\sqrt{3}}, \frac{4(\sqrt{3}-1)}{3}, \frac{4}{3} \right)$$

as also verified by a fast numerical simulation (see Fig.9)

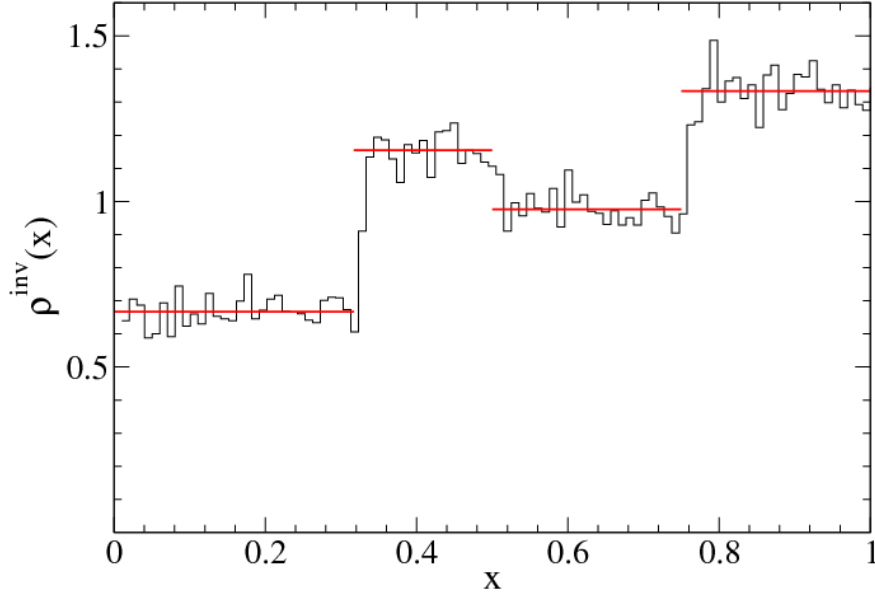


FIG. 9: Invariant distribution of the roof map from a long trajectory compared with the analytical solution of obtained by Perron-Frobenius operator (horizontal lines).

## CHAPTER 5: Characterization of Chaotic Dynamical Systems

### Exercise 5.1

Consider the subset  $A$ , of the interval  $[0:1]$ , whose elements are the infinite sequence of points:

$$A = \left\{ 1, \frac{1}{2^\alpha}, \frac{1}{3^\alpha}, \frac{1}{4^\alpha}, \dots, \frac{1}{n^\alpha}, \dots \right\}$$

with  $\alpha > 0$ . Show that the Box-counting dimension  $D_F$  of set  $A$  is  $D_F = 1/(1 + \alpha)$ .

### Solution

Let  $x_n = n^{-\alpha}$  be the  $n$ -th point of the sequence  $A$  and introduce  $\epsilon_n = x_n - x_{n+1}$ . For  $n$  sufficiently large, we have  $\epsilon_n \sim \alpha/n^{\alpha+1}$ . Each element of  $\{x_n\}_{n=0}^\infty$  is contained in the interval  $[0:1]$ . Given  $n = N$ , we can divide the set of points in two sets those such that  $x_i < x_N$  and those for which  $x_i \geq x_N$ . In the second set, the distance between successive points  $x_i - x_{i+1}$  is larger than  $\epsilon_N$ . Therefore, we need a number of boxes  $N^{(2)}(\epsilon_N)$  proportional to the number of points in  $[x_N:1]$  to be covered, i.e.  $N^{(2)}(\epsilon_N) \sim N$ . While to cover the points in first set, which are contained in the interval  $[0:x_N]$ , we need a number  $N^{(1)}(\epsilon_N) \sim x_N/\epsilon_N \sim N$  of boxes. The global number of  $\epsilon_N$ -boxes is thus

$$N^{(1)} + N^{(2)} \sim N \sim \epsilon_N^{-1/(1+\alpha)}$$

from which we obtain  $D_F = 1/(1 + \alpha)$ .

### Exercise 5.2

Show that the invariant set (repeller) of the map

$$x(t+1) = f(x(t)) = \begin{cases} 3x(t) & \text{if } 0 \leq x(t) < 1/2; \\ 3(1-x(t)) & \text{if } 1/2 \leq x(t) \leq 1. \end{cases}$$

is the Cantor set discussed in Sec. 5.2 with fractal dimension  $D_F = \ln(2)/\ln(3)$ .

### Solution

The map is defined in the unit interval  $[0:1]$ , therefore all points  $y$  such that  $f(y) > 1$  are expelled from the system dynamics. Looking at the graph of the map and the second iterate

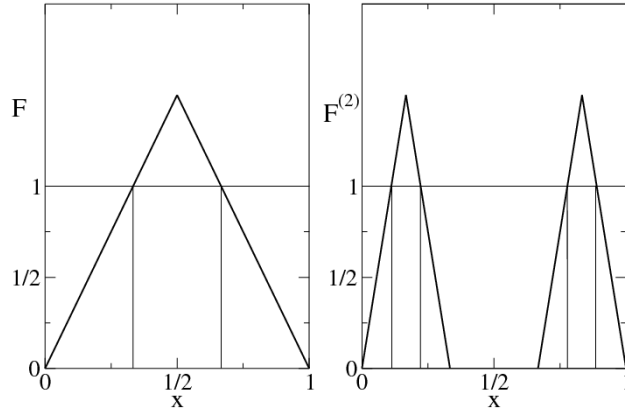


FIG. 10: Plot of the repeller map of Ex.5.2

of the map (Fig.10) it is rather easy to see that after the first iteration the only points which remain are those belonging to  $[0 : 1/3] \cup [2/3 : 1]$ . Then after two iterations those form the set  $[0 : 1/9] \cup [2/9 : 1/2] \cup [2/3 : 2/3 + 1/9] \cup [2/3 + 2/9 : 1]$  and so on. In other terms, at each iteration one erases the central third of the intervals of the previous step. Consequently, after an infinite number of iteration the set of points remaining in the unit interval is just the Cantor set, whose fractal dimension was computer in Ch.5.

### Exercise 5.3

*Numerically compute the Grassberger-Procaccia dimension for:*

- (1) Hénon attractor obtained with  $a = 1.4, b = 0.3$ ;
- (2) Feigenbaum attractor obtained with logistic map at  $r = r_\infty = 3.569945\dots$

### Exercise 5.4

*Consider the following two-dimensional map*

$$\begin{aligned} x(t+1) &= \lambda_x x(t) \quad \text{mod } 1 \\ y(t+1) &= \lambda_y y(t) + \cos(2\pi x(t)) \end{aligned} \tag{7}$$

$\lambda_x$  and  $\lambda_y$  being positive integers with  $\lambda_x > \lambda_y$ . This map has no attractors with finite  $y$ , as almost every initial condition generates an orbit escaping to  $y = \pm\infty$ . Show that:



1. the basins of attraction boundary is given by the Weierstrass' curve [Falconer (2003)] defined by

$$y = - \sum_{n=1}^{\infty} \lambda_y^{-n} \cos(2\pi \lambda_x^{n-1} x);$$

2. the fractal dimension of such a curve is  $D_F = 2 - \frac{\ln \lambda_y}{\ln \lambda_x}$  with  $1 < D_F < 2$ .

### Solution

1) Let  $y = F(x)$  indicate the function which separates the two basins of attraction at  $\pm\infty$ . By definition  $y = F(x)$  is invariant under the evolution of the map (7), that is, if  $y(t) = F(x(t))$  then  $y(t+1) = F(x(t+1))$  for any  $t$ .

Let us expand  $F(x)$  in Fourier series

$$y = F(x) = \sum_{n=0}^{\infty} a_n \cos(2\pi k_n x). \quad (*)$$

By denoting with  $(x', y')$  the first iterate of  $(x, y)$  under the map (7) we have

$$F(x') = \sum_{n=0}^{\infty} a_n \cos(2\pi k_n \lambda_x x) = y' = \lambda_y y + \cos(2\pi x)$$

substituting  $y$  from (\*) we obtain the identity

$$\sum_{n=0}^{\infty} a_n \cos(2\pi k_n \lambda_x x) = \sum_{n=0}^{\infty} \lambda_y a_n \cos(2\pi k_n x) + \cos(2\pi x)$$

from which, identifying the homologous terms in the series, we can determine the coefficients  $a_n$  and the wave numbers  $k_n$ . In particular, we have

$$a_0 \cos(2\pi k_0 \lambda_x x) + a_1 \cos(2\pi k_1 \lambda_x x) + \dots = \lambda_y a_0 \cos(2\pi k_0 x) + \lambda_y a_1 \cos(2\pi k_1 x) + \dots + \cos(2\pi x).$$

and thus  $k_0 = 1$ ,  $a_0 = -1/\lambda_y$ ,

$$k_1 = k_0 \lambda_x, \quad a_1 = a_0 / \lambda_y$$

⋮

$$k_n = k_0 \lambda_x^n, \quad a_n = a_0 / \lambda_y^n.$$

These relationships provide the result:

$$y = - \sum_{n=1}^{\infty} \lambda_y^{-n} \cos(2\pi \lambda_x^{n-1} x);$$

Fig.11 illustrates how the curve looks like for a couple of values for  $\lambda_{x,y}$ .

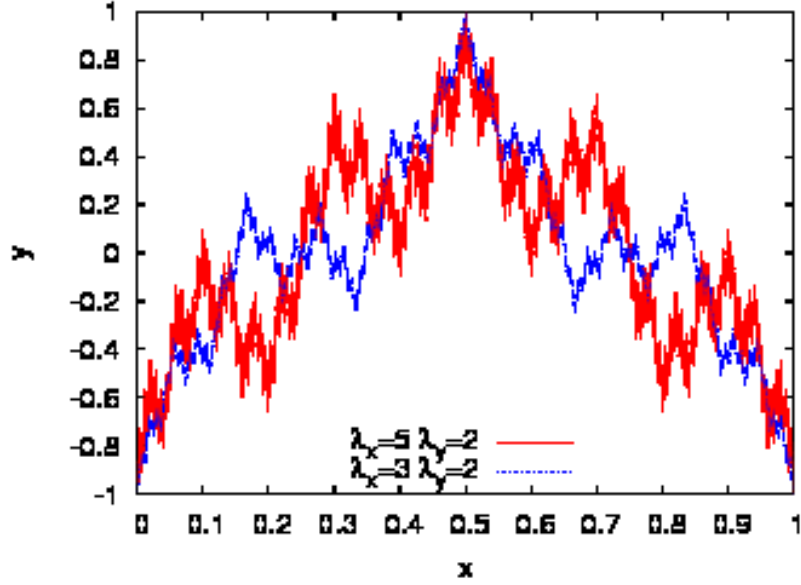


FIG. 11: Plot of the repeller map of Ex.5.2.

2) Let us now compute the fractal dimension  $D_F$  of such a curve.

In order to find  $D_F$  consider  $\Delta F(\Delta x) = F(x + \Delta x) - F(x)$  and analyze the small  $\Delta x$  scaling:  $\Delta F \sim \Delta x^\alpha$ , one has  $\alpha = 2 - D_F$ . Indeed if we want to cover a fragment of curve within an interval  $[x : x + \Delta x]$  we need  $\Delta x^{\alpha-1}$  boxes, and the whole curve being in  $x \in [0 : 1]$  we need in total  $(1/\Delta x)\Delta x^{\alpha-1} = \Delta x^{-(2-\alpha)} = \Delta x^{-D_F}$  boxes. Therefore, we just need to know  $\alpha$ .

If  $\Delta x \sim \lambda_x^{-n}$ , the leading contribution to  $\Delta F$  is  $\mathcal{O}(a_n)$  therefore

$$\Delta F(\Delta x \sim \lambda_x^{-n}) \sim \lambda_y^{-n}$$

and by writing  $\lambda_y = \lambda_x^{\ln(\lambda_y)/\ln(\lambda_x)}$ , we obtain the result

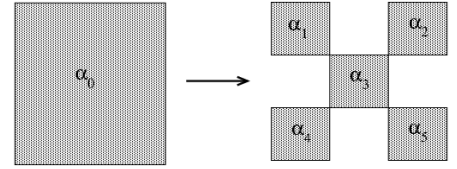
$$\Delta F \sim \lambda_x^{-n \ln(\lambda_y)/\ln(\lambda_x)} \sim \Delta x^{\ln(\lambda_y)/\ln(\lambda_x)}.$$

and finally

$$D_F = 2 - \frac{\ln(\lambda_y)}{\ln(\lambda_x)}$$

**Exercise 5.5**

Consider the fractal set  $A$  generated by infinite iteration of the geometrical rule of basic step as in the figure on the right. We define a measure on this fractal as follows: let  $\alpha_1, \dots, \alpha_5$  be positive numbers such that  $\sum_{i=1}^5 \alpha_i = 1$ . At the first stage of the construction, we assign to the upper-left box the measure  $\alpha_1$ ,  $\alpha_2$  to the upper-right box and so on, as shown in the figure. Compute the dimension  $D(q)$ .



**Solution**

The geometrical construction at the  $n$ -th generation suggests to consider a covering with square boxes of side  $\ell_n$ . Let us introduce the two quantities

$$\ell_n = \frac{\ell_0}{3^n} = \frac{\ell_{n-1}}{3}$$

$$M_n(q) = \sum_j^{(n)} P_j(\ell_n)^q$$

where the summation symbol  $\sum_j^{(n)}$  indicates that the sum runs over the non-empty boxes of size  $\ell_n$  only.

Note that each box  $j'$ , at scale  $\ell_{n+1}$ , is obtained from a box  $j$  at scale  $\ell_n$ :

$$P_{j'}(\ell_{n+1}) = \alpha_k P_j(\ell_n)$$

therefore we have:

$$M_{n+1}(q) = \sum_{j'}^{(n+1)} P_{j'}(\ell_{n+1})^q = \sum_{k=1}^5 \alpha_k^q \sum_j^{(n)} P_j(\ell_n)^q$$

the formula can be recast so to obtain the simple iteration rule:

$$M_{n+1}(q) = \left( \sum_{k=1}^5 \alpha_k^q \right) M_n(q)$$

whose solution is  $M_n(q) \sim (\sum_{k=1}^5 \alpha_k^q)^n$  which, in turn, leads to the generalized fractal dimension

$$D(q) = \frac{1}{1-q} \frac{\ln(\sum_{k=1}^5 \alpha_k^q)}{\ln(3)}.$$

For  $q \rightarrow 0$ , we obtain the fractal dimension  $D(0) = \ln 5 / \ln 3$ .

**Exercise 5.6**

Compute the Lyapunov exponents of the two-dimensional map:

$$\begin{aligned}x(t+1) &= \lambda_x x(t) + \sin[2\pi y(t)^2] && \text{mod } 1 \\y(t+1) &= 4y(t)[1 - y(t)]\end{aligned}$$

**Solution**

We can start linearizing the map

$$\begin{pmatrix} \delta x(t+1) \\ \delta y(t+1) \end{pmatrix} = \begin{pmatrix} \lambda_x & 4\pi y(t) \cos(2\pi y^2(t)) \\ 0 & 4 - 8y(t) \end{pmatrix} \cdot \begin{pmatrix} \delta x(t) \\ \delta y(t) \end{pmatrix} \quad (8)$$

The triangular structure of the matrix is preserved under matrix multiplication, meaning that the product is still a triangular matrix. Furtherly, the  $y$ -dynamics does not depend on the  $x$ -dynamics. So that the two Lyapunov exponents are simply  $\ln(2)$  associated to logistic map  $4y(t)[1 - y(t)]$  and  $\ln|\lambda_x|$  as under matrix multiplication the first element will be  $\lambda_x^n$ .

**Exercise 5.7**

Consider the two-dimensional map defined by the equations

$$\begin{aligned}x(t+1) &= 2x(t) && \text{mod } 1 \\y(t+1) &= ay(t) + 2\cos(2\pi x(t))\end{aligned}$$

a) Show that if  $|a| < 1$  there exists a finite attractor. b) Compute the Lyapunov exponents  $\lambda_1, \lambda_2$ .

**Solution**

a) The motion occurs on a finite attractor when there exists a constant  $c > 0$  such that if  $|y(t)| < c$  then  $|y(t+1)| < c$  too. As we have that

$$|y(t+1)| = |ay(t) + 2\cos(2\pi x(t))| \leq |a||y(t)| + 2.$$

now if we require  $|y(t+1)| < c$ , implying the inequality  $|a||y(t)| + 2 < c$  and thus  $c > 2(1 - |a|)$ , which is positive as long as  $|a| < 1$ .

b) With the same argument of Ex.5.6, we obtain  $\lambda_1 = \ln(2)$  and  $\lambda_2 = \ln|a| < 0$ .

### Exercise 5.8

Numerically compute the Lyapunov exponents  $\{\lambda_1, \lambda_2\}$  of the Hénon map for  $a = 1.4, b = 0.3$ , check that  $\lambda_1 + \lambda_2 = \ln b$ ; and test the Kaplan-Yorke conjecture with the fractal dimension computed in Ex.5.3

**Hint:** Evolve the map together with the tangent map, use Gram-Schmidt orthonormalization trying different values for the number of steps between two successive orthonormalization.

### Exercise 5.9

Numerically compute the Lyapunov exponents for the Lorenz model. Compute the whole spectrum  $\{\lambda_1, \lambda_2, \lambda_3\}$  for  $r = 28, \sigma = 10, b = 8/3$  and verify that:  $\lambda_2 = 0$  and  $\lambda_3 = -(\sigma + b + 1) - \lambda_1$ .

**Hint:** Solve first Ex.5.8, check the dependence on the time and orthonormalization step.

### Exercise 5.10

Numerically compute the Lyapunov exponents for the Hénon-Heiles system. Compute the whole spectrum  $\{\lambda_1, \lambda_2, \lambda_3, \lambda_4\}$ , for trajectory starting from an initial condition in “chaotic sea” on the energy surface  $E = 1/6$ . Check that:  $\lambda_2 = \lambda_3 = 0; \lambda_4 = -\lambda_1$ .

**Hint:** Do not forget that the system is conservative, check the conservation of energy during the simulation.

### Exercise 5.11

Consider the one-dimensional map defined as follows

$$x(t+1) = \begin{cases} 4x(t) & 0 \leq x(t) < \frac{1}{4} \\ \frac{4}{3}(x(t) - 1/4) & \frac{1}{4} \leq x(t) \leq 1. \end{cases}$$

Compute the generalized Lyapunov exponent  $L(q)$  and show that:

(1)  $\lambda_1 = \lim_{q \rightarrow 0} L(q)/q = \ln 4/4 + 3/4 \ln(4/3);$

(2)  $\lim_{q \rightarrow \infty} L(q)/q = \ln 4;$

(3)  $\lim_{q \rightarrow -\infty} L(q)/q = \ln(4/3).$

Finally, compute the Cramer function  $S(\gamma)$  for the effective Lyapunov exponent.

### Solution

It is rather easy to realize that this map has invariant measure  $\rho_{inv} = 1$  in  $[0 : 1]$ . Moreover, the derivative of the map has only two values. Therefore, the tangent evolution  $\delta x(t+1) = f'[x(t)]\delta x(t)$  is characterized by only two multipliers 4 and  $4/3$  occurring with probability  $p_1 = 1/4$  and  $p_2 = 3/4$ , respectively, i.e.:

$$\delta x(t+1) = \begin{cases} 4\delta x(t) & x \in [0:1/4[ \\ 4/3\delta x(t) & x \in [1/4:1] \end{cases} . \quad (9)$$

We thus have that  $R(t) = |\delta x(t)|$  evolves according to

$$R(t+1) = \begin{cases} 4R(t) & \text{with prob. } p_1 \\ 4/3R(t) & \text{with prob. } p_2 \end{cases} ,$$

from which we derive the recursion for the  $q$ -moments  $\langle R(t)^q \rangle$  of  $R$ :

$$\langle R(t+1)^q \rangle = \langle R(t)^q \rangle \left[ p_1 4^q + p_2 \left( \frac{4}{3} \right)^q \right]$$

which is solved as  $\langle R(t)^q \rangle \sim [p_1 4^q + p_2 (4/3)^q]^t$ . The generalized Lyapunov exponent

$$L(q) = \lim_{t \rightarrow \infty} \frac{1}{t} \ln \langle R(t)^q \rangle$$

are thus given by the formula

$$L(q) = \ln \left\{ 4^{q-1} + \left( \frac{4}{3} \right)^{q-1} \right\} .$$

Let us now consider the questions (1) (2) and (3).

(1) By expanding  $L(q)$  to first order in  $q$  we obtain

$$L(q) \simeq q \left\{ \frac{1}{4} \ln(4) + \frac{3}{4} \ln \left( \frac{4}{3} \right) \right\} \longrightarrow \lambda_1 = \frac{1}{4} \ln(4) + \frac{3}{4} \ln \left( \frac{4}{3} \right)$$

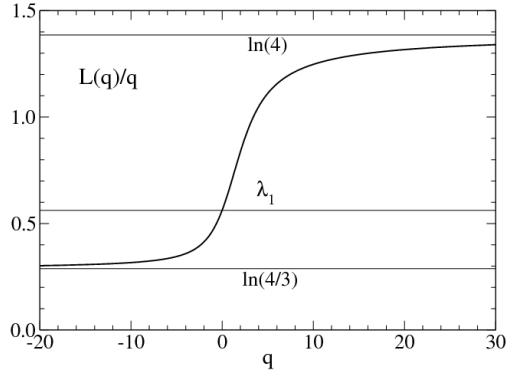


FIG. 12: Plot of  $L(q)$  vs  $q$  for the map (9) set A.

moreover

$$L(q) \simeq \begin{cases} q \ln 4 & \text{if } q \rightarrow \infty \\ q \ln(4/3) & \text{if } q \rightarrow -\infty. \end{cases}$$

Let us now compute the Cramer function. We recall that the effective Lyapunov exponent is defined as  $\gamma(t) = 1/t \ln R(t)$ , its finite time character makes it a fluctuating quantity. In the case of the map considered it can be written as:

$$\gamma(t) = \frac{1}{t} \sum_{i=1}^t \xi_i$$

where

$$\xi_i = \begin{cases} a = \ln 4 & \text{with prob. } p_1 \\ b = \ln(4/3) & \text{with prob. } p_2 \end{cases}$$

with  $p_1 = 1/4$ ,  $p_2 = 3/4$ . The above equation defines a Benoulli process with outcomes  $(a, b)$  and probability  $(p_1, 1 - p_1)$ . In order to compute probability that  $\gamma(t) = \gamma$ , it is necessary to know the number  $k$  of the outcome  $a$  in a total of  $t$  iterates,

$$\gamma(t) = \frac{ak + b(t - k)}{t} = af + b(1 - f) \quad (10)$$

where  $f = k/t$  is the occurrence frequency of the outcome  $\xi = a$  in  $t$  trials. The probability to have  $k$  events in  $t$  trials is given by a Bernoulli distribution:

$$P_t(k) = \binom{k}{t} p_1^k (1 - p_1)^{t-k}$$

that by using, in the limit  $t$  large, the Stirling formula and in term of the variable  $f$  becomes:

$$P_t(f) \sim \exp \left\{ -t \left[ f \ln \left( \frac{f}{p_1} \right) + (1-f) \ln \left( \frac{1-f}{1-p_1} \right) \right] \right\}.$$

Now, recalling Eq. (10), we can change the variable  $f = (\gamma - b)/(a - b)$  to obtain the distribution for  $\gamma$

$$P_t(\gamma) \sim \exp \left\{ -t \left[ \frac{\gamma - b}{a - b} \ln \left( \frac{\gamma - b}{p_1(a - b)} \right) + \frac{a - \gamma}{a - b} \ln \left( \frac{a - \gamma}{(1 - p_1)(a - b)} \right) \right] \right\}.$$

then the Cramer's function is:

$$S(\gamma) = \frac{\gamma - b}{a - b} \ln \left( \frac{\gamma - b}{p_1(a - b)} \right) + \frac{a - \gamma}{a - b} \ln \left( \frac{a - \gamma}{(1 - p_1)(a - b)} \right).$$

which means

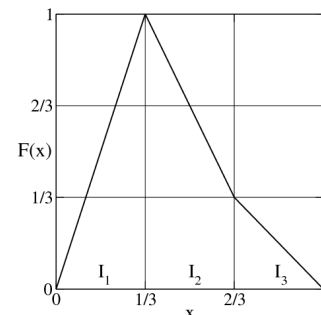
$$S(\gamma) = \frac{\gamma - \ln(4/3)}{\ln 3} \ln \frac{4\gamma - 4 \ln(4/3)}{\ln 3} + \frac{\ln 4 - \gamma}{\ln 3} \ln \frac{4 \ln 4 - 4\gamma}{3 \ln 3}.$$

### Exercise 5.12

Consider the one-dimensional map

$$x(t+1) = \begin{cases} 3x(t) & 0 \leq x(t) < 1/3 \\ 1 - 2(x(t) - 1/3) & 1/3 \leq x(t) < 2/3 \\ 1 - x(t) & 2/3 \leq x(t) \leq 1 \end{cases}$$

illustrated on the right. Compute the LE and the generalized LE.

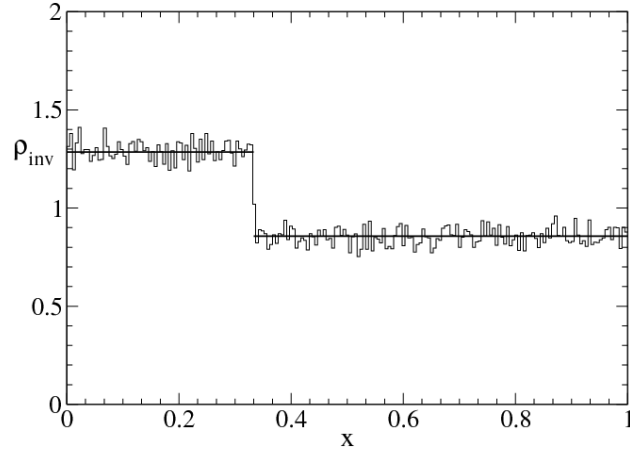


### Solution

It is easy to realize that the partition of the interval  $[0:1]$  of sets  $I_1 = [0:1/3]$ ,  $I_2 = [1/3:2/3]$  and  $I_3 = [2/3:1]$  is a Markov partition and that the invariant measure is defined by a density  $\rho_{inv}(x)$  constant in each interval:

$$\rho_{inv}(x) = \begin{cases} \rho_1 & x(t) \in I_1 \\ \rho_2 & x(t) \in I_2 \\ \rho_3 & x(t) \in I_3 \end{cases}$$





The constants  $\rho_1, \rho_2, \rho_3$  are determined according to the transition probability matrix, indicating how the dynamics determines statistically the transitions among the sets  $I$ :

$$P_{1 \rightarrow 1} = P_{1 \rightarrow 2} = P_{1 \rightarrow 3} = 1/3,$$

$$P_{2 \rightarrow 1} = 0, P_{2 \rightarrow 2} = 1/2, P_{2 \rightarrow 3} = 1/2$$

$$P_{3 \rightarrow 1} = 1, P_{3 \rightarrow 2} = P_{3 \rightarrow 3} = 0 .$$

The equation for the invariant distribution is

$$\begin{aligned} \rho_1 &= \frac{1}{3}\rho_1 + \rho_3 \\ \rho_2 &= \frac{1}{3}\rho_1 + \frac{1}{2}\rho_2 \\ \rho_3 &= \frac{1}{3}\rho_1 + \frac{1}{2}\rho_2 \end{aligned}$$

admits the solution  $\rho_{inv} = (9/7, 6/7, 6/7)$ . The formula for the Lyapunov exponent is  $\lambda_1 = \langle \ln |f'(x)| \rangle$  where the average is on  $\rho_{inv}(x)$ . The map has three constant slopes

$$f'(x) = \begin{cases} 3 & x(t) \in I_1 \\ -2 & x(t) \in I_2 \\ -1 & x(t) \in I_3 \end{cases}$$

thus the direct application of this formula gives

$$\lambda_1 = \frac{3}{7} \ln 3 + \frac{2}{7} \ln 2$$

$L(q)$  can be computed as in Ex.5.11.

## CHAPTER 6: From Order to Chaos in Dissipative Systems

### Exercise 6.1

Consider the system

$$\frac{dx}{dt} = y, \quad \frac{dy}{dt} = z^2 \sin x \cos x - \sin x - \mu y, \quad \frac{dz}{dt} = k(\cos x - \rho)$$

with  $\mu$  as control parameter. Assume that  $\mu > 0$ ,  $k = 1$ ,  $\rho = 1/2$ . Describe the bifurcation of the fixed points at varying  $\mu$ .

### Solution

The fixed points of the system are the solution of

$$\begin{aligned} y &= 0 \\ \sin(x) \cos(x) z^2 - \sin(x) - \mu y &= 0 \\ \cos(x) - \rho &= 0 \end{aligned}$$

which implies two fixed points  $P_{\pm} = (x^*, y^*, z^*) = (\arccos(\rho), 0, \pm 1/\sqrt{\rho})$ . When  $\rho = 1/2$  and  $k = 1$ , the stability matrix evaluated on  $P_{\pm} = (\pi/3, 0, \pm\sqrt{2})$  reads

$$\begin{pmatrix} 0 & 1 & 0 \\ -3/2 & -\mu \pm \sqrt{3}/2 & \\ -\sqrt{3}/2 & 0 & 0 \end{pmatrix}$$

from which the secular equation is

$$\lambda^3 + \mu\lambda^2 + \frac{3}{2}\lambda \mp \frac{3}{2\sqrt{2}} = 0. \quad (11)$$

Clearly, the fixed point  $P_-$  is always unstable, because the determinant of the stability matrix is positive, indicating the presence of at least one eigenvalue with positive real part. Therefore, we can limit our analysis to  $P_+$ .

The stability condition requires that none of the roots have a positive real part. This can be checked using the Routh-Hurwitz criterion (Gantmaker *Matrix Theory* American Mathematical Society (1990)). According to this criterion, the Characteristic Polynomial

$P(\lambda) = a_0\lambda^3 + a_1\lambda^2 + a_2\lambda + a_3$  has no roots with positive  $Re(\lambda)$  if and only if the matrix

$$\begin{pmatrix} a_1 & a_3 & 0 \\ a_0 & a_2 & 0 \\ 0 & a_1 & a_3 \end{pmatrix} = \begin{pmatrix} \mu & \frac{3}{2\sqrt{2}} & 0 \\ 1 & \frac{3}{2} & 0 \\ 0 & \mu & \frac{3}{2\sqrt{2}} \end{pmatrix}$$

has positive determinants of minors, i.e. if

$$\Delta_1 = a_1 = \mu > 0,$$

$$\Delta_2 = \det \begin{pmatrix} a_1 & a_3 \\ a_0 & a_2 \end{pmatrix} = \frac{3\mu}{2} - \frac{3}{2\sqrt{2}} > 0,$$

$$\Delta_3 = \det \begin{pmatrix} a_1 & a_3 & 0 \\ a_0 & a_2 & 0 \\ 0 & a_1 & a_3 \end{pmatrix} = \frac{3\mu}{2\sqrt{2}} - \frac{9}{8} > 0.$$

The above disequalities are simultaneously satisfied for  $\mu > 1/\sqrt{2}$ , therefore for  $\mu > \mu_c$  the fixed point  $P_+$  is always stable, while below  $\mu_c$  a change of stability occurs, meaning that at the critical point  $\mu_c = 1/\sqrt{2}$ , the real part of at least one of the eigenvalues crosses the zero. A possibility is that two complex conjugate eigenvalues crosses the imaginary axis as in Hopf bifurcation. In the following, we check such a possibility.

If we look for solutions with one real and two pure imaginary eigenvalues, i.e.  $\lambda_1$  and  $\pm i\omega$ , then the equation should factorize to  $(\lambda - \lambda_1)(\lambda^2 + \omega^2) = 0$ . Expanding we obtain

$$\lambda^3 - \lambda_1\lambda^2 + \omega^2\lambda - \lambda_1\omega^2 = 0.$$

Now comparing to Eq. (11) with  $\mu = \mu_c = 1/\sqrt{2}$  we have  $\lambda_1 = -\mu_c$ ,  $\omega^2 = 3/2$ ,  $\lambda_1\omega^2 = \pm 3/(2\sqrt{2})$ , i.e. one of the hypothesis of Hopf bifurcation is verified.

Now, we have to check for the transversality condition at  $\mu_c$ , i.e.

$$\frac{d\Re\{\lambda\}}{d\mu} \neq 0.$$

To do so, we can differentiate Eq. (11) with respect to  $\mu$

$$3\lambda^2 \frac{d\lambda}{d\mu} + \lambda^2 + 2\mu\lambda \frac{d\lambda}{d\mu} + \frac{3}{2} \frac{d\lambda}{d\mu} = 0$$

then solving for the derivative:

$$\left. \frac{d\lambda}{d\mu} \right|_{\mu_c} = -\frac{\lambda^2(\mu_c)}{3\lambda^2(\mu_c) + 2\mu_c\lambda(\mu_c) + 3/2}.$$

For the two complex conjugated eigenvalues  $\lambda_{2,3} = \alpha \pm i\omega$ , at  $\mu_c = 1/\sqrt{2}$  (considering that  $\alpha(\mu_c) = 0$  and  $\omega^2 = 3/2$ )

$$\left. \frac{d\lambda_{2,3}}{d\mu} \right|_{\mu_c} = \frac{\omega^2}{-3\omega^2 \pm i2\mu_c\omega + 3/2} = -\frac{3/2}{3 \mp i\sqrt{3}}$$

then the derivative of the real part of  $\lambda_{2,3}$  is  $-3/4$ , not vanishing at  $\mu_c$ .

Finally, in order to demonstrate that transition is Hopf, we need to verify also the condition that the fixed point  $P_+$  is a *vague attractor*, i.e. initial conditions in a neighborhood of  $P_+$  are attracted, thanks to the nonlinear terms, by the fixed point. There is no general technique to test the existence of a vague attractor and it is in general very difficult to prove it. So that, often, one has to resort to numerical studies, in this case we suggest to study numerically the trajectories behavior close to the transition.

## Exercise 6.2

Consider the set of ODEs

$$\frac{dx}{dt} = 1 - (b+1)x + ax^2y, \quad \frac{dy}{dt} = bx - ax^2y$$

known as Brusselator which describes a simple chemical reaction.

- (1) Find the fixed points and study their stability.
- (2) Fix  $a$  and vary  $b$ . Show that at  $b_c = a+1$  there is a Hopf bifurcation and the appearance of a limit cycle.
- (3) Estimate the dependence of the period of the limit cycle as a function of  $a$  close to  $b_c$ .

## Solution

- 1) The fixed points are solutions of the equations

$$\begin{aligned} 1 - (b+1)x + ax^2y &= 0 \\ bx - ax^2y &= 0 \end{aligned}$$

that means  $P = (1, b/a)$ . The stability of  $P$  is determined by the eigenvalues of the stability matrix

$$\mathbb{L} = \begin{pmatrix} b-1 & a \\ -b & -a \end{pmatrix}$$

$\lambda_{1,2} = 1/2[b-1-a \pm \sqrt{-4a+(1+a-b)^2}]$ , clearly the stability will depend on the values of  $a$  and  $b$ . We can easily understand the main stability features considering the trace and determinant of the stability matrix. In particular,  $Tr(\mathbb{L}) = \lambda_1 + \lambda_2 = b-1-a$  and  $\det(\mathbb{L}) = \lambda_1\lambda_2 = a$ . Let us consider, e.g., the case  $a > 0$  which means  $\lambda_1$  and  $\lambda_2$  have the same sign, which is determined by the trace:  $\lambda_1, \lambda_2 > 0$  (and thus the point is a repeller) if  $b > 1+a$  while  $\lambda_1, \lambda_2 < 0$  (and thus the point is an attractor repeller) if  $b < 1+a$ . When  $a < 0$  the signs is different and we can have hyperbolic points.

2) A Hopf bifurcation, at fixed  $a$  and varying  $b$ , requires that both eigenvalues becomes pure imaginary, that means that the real part has to be zero, i.e.  $b-1-a=0$ , and simultaneously the determinant  $\Delta = -a$  must be negative. Of course, this implies  $b_c = 1+a$  and  $\Delta = -a < 0$  for  $a > 0$ . In order for the bifurcation to be of type Hopf we also need to prove that the derivative of the real part is non zero at  $b = b_c$ , i.e. we need to evaluate

$$\frac{\partial Re\{\lambda\}}{\partial b} = 1/2 \neq 0$$

as required. This confirms that for  $a > 0$  at  $b = b_c$  we have a Hopf bifurcation.

Finally, in order to demonstrate that transition is Hopf, we need to verify also the condition that the fixed point is a *vague attractor*. Similarly to the previous exercise we suggest a numerical investigation close to the critical point.

3) At  $b = b_c$  the eigenvalues are pure imaginary  $\lambda = \pm i\omega = \pm i\sqrt{a}$  so that the period will be  $T \sim 2\pi/\sqrt{a}$ .

### Exercise 6.3

*Estimate the Feigenbaum constants of the sin map Ex.3.3 from the first, say 4, 6 period doubling bifurcations and see how they approach the known universal values.*

#### Exercise 6.4

Consider the logistic map at  $r = r_c - \epsilon$  with  $r_c = 1 + \sqrt{8}$  (see also Eq. (3.2)). Graphically study the evolution of the third iterate of the map for small  $\epsilon$  and, specifically, investigate the region close to  $x = 1/2$ . Is it similar to the Lorenz map for  $r = 166.3$ ? Why? Expand the third iterate of the map close to its fixed point and compare the result with Eq. (6.11). Study the behavior of the correlation function at decreasing  $\epsilon$ . Do you have any explanation for its behavior?

#### Solution

Reconsider Ex.3.2.

#### Exercise 6.5

Consider the one-dimensional map defined by

$$F(x) = x_c - (1 + \epsilon)(x - x_c) + \alpha(x - x_c)^2 + \beta(x - x_c)^3 \pmod{1}$$

(1) Study the change of stability of the fixed point  $x_c$  at varying  $\epsilon$ , in particular perform the graphical analysis using the second iterate  $F(F(x))$  for  $x_c = 2/3$ ,  $\alpha = 0.3$  and  $\beta = \pm 1.1$  at increasing  $\epsilon$ , what is the difference between the  $\beta > 0$  and  $\beta < 0$  case?

(2) Consider the case with negative  $\beta$  and iterate the map comparing the evolution with that of the map (6.11)

The kind of behavior displayed by this map has been termed intermittency of III-type (see sec:4.2.5).

## CHAPTER 7: Chaos in Hamiltonian Systems

### Exercise 7.1

Consider the standard map

$$\begin{aligned}I(t+1) &= I(t) + K \sin(\theta(t)) \\ \theta(t+1) &= \theta(t) + I(t+1) \pmod{2\pi},\end{aligned}$$

write a numerical code to compute the action diffusion coefficient

$D = \lim_{t \rightarrow \infty} \frac{1}{2t} \langle (I(t) - I_0)^2 \rangle$  where the average is over a set of initial values  $I(0) = I_0$ . Produce a plot of  $D$  versus the map parameter  $K$  and compare the result with Random Phase Approximation, consisting in assuming  $\theta(t)$  as independent random variables, which gives  $D_{RPA} = K^2/4$  [Lichtenberg and Liebermann (1992)]. Note that for some specific values of  $K$  (e.g  $K = 6.9115$ ) the diffusion is anomalous, since the mean square displacement scales with time as  $\langle (I(t) - I_0)^2 \rangle \sim t^{2\nu}$ , where  $\nu > 1/2$  (see Castiglione et al (1999)).

### Hints and Solution

To compute  $D$  numerically, at each value of  $K$ , one has to simulate the map for many different initial conditions over a reasonably long time so to estimate:

$$\frac{\langle (I(t) - I(0))^2 \rangle}{2t}. \quad (**)$$

The RPA consists in assuming that the angle  $\theta$  is a random variable in  $[0:2\pi]$ , assuming no correlation we have that the approximate diffusion coefficient can be estimated from a single step, i.e. by the following ratio

$$D_{RPA} = \frac{1}{2} \langle (I(t+1) - I(t))^2 \rangle = \frac{K^2}{4\pi} = \int_0^{2\pi} \sin^2 \theta d\theta = \frac{K^2}{4}.$$

Of course correlations and different distribution for the angle should be considered in the true problem, these are responsible for the differences between the result of numerical simulations and the RPA approximation.

In Fig.13 we show a comparison between RPA and numerical simulations of the quantity  $(**)$  computed with  $t = 1000$  and  $10^4$  initial conditions. Note also the pronounced peaks for some values of  $K$ , looking around them one can discover the presence of anomalous diffusion. Repeating the simulations with different values of  $t$  one has that these peaks increase with  $t$ , which is the signature of anomalous diffusion.

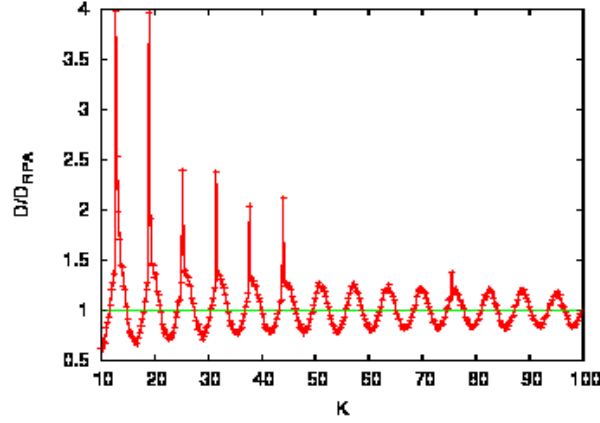


FIG. 13: Ratio between the numerically determined diffusion coefficient and  $D_{RPA}$ .

### Exercise 7.2

Using some numerical algorithm for ODE to integrate the Duffing oscillator (7.15) Check that for small  $\epsilon$

- (1) trajectories starting from initial conditions close to the separatrix have  $\lambda_1 > 0$ ;
- (2) trajectories with initial conditions far enough from the separatrix exhibit regular motion ( $\lambda_1 = 0$ ).

### Exercise 7.3

Consider the time-dependent Hamiltonian

$$H(q, p, t) = -V_2 \cos(2\pi p) - V_1 \cos(2\pi q)K(t) \quad \text{with} \quad K(t) = \tau \sum_{n=-\infty}^{\infty} \delta(t - n\tau)$$

called the kicked Harper model. Show that integrating over the time of a kick (as for the standard map in Sec 2.2.1.2) it reduces to the Harper map

$$p(n+1) = p(n) - \gamma_1 \sin(2\pi q(n))$$

$$q(n+1) = q(n) + \gamma_2 \sin(2\pi p(n+1)),$$

with  $\gamma_i = 2\pi V_i \tau$ , which is symplectic. For  $\tau \rightarrow 0$  this is an exact integration of the original Hamiltonian system. Fix  $\gamma_{1,2} = \gamma$  and study the qualitative changes of the dynamics as  $\gamma$  becomes larger than 0. Find the analogies with the standard map, if any.



## Solution

The Hamiltonian is of the form

$$H(q, p, t) = T(p) + V(q)K_\tau(t)$$

with  $K_\tau(t)$  composed by  $\delta$ -kicks having period  $\tau$ . The associated Hamilton equations are:

$$\begin{aligned}\frac{dp}{dt} &= -\frac{dV}{dq} = V'(q) = -V_1 2\pi \sin(2\pi q)K(t) \\ \frac{dq}{dt} &= \frac{dT}{dp} = T'(p) = V_2 2\pi \sin(2\pi p)\end{aligned}$$

from the first equation it is clear that  $p$  is constant between two kicks, while  $q$  increases linearly between the kicks with a slope determined by the value of  $p$  in that interval. Let  $p(n)$  and  $q(n)$  denote the value of  $p(t)$  and  $q(t)$  at  $t = n\tau + 0^-$  (i.e. right before the kick).

Integrating the first Hamilton equation in  $[n\tau : (n+1)\tau]$  we have

$$p(n+1) - p(n) = \int_{n\tau+0^-}^{(n+1)\tau+0^-} \frac{dp}{dt} dt = -V'(q(n))$$

while the second equation gives

$$q(n+1) - q(n) = \int_{n\tau+0^-}^{(n+1)\tau+0^-} \frac{dq}{dt} dt = T'(p(n+1))$$

so that the resulting discrete time dynamics assume the form

$$\begin{aligned}p(n+1) &= p(n) - V'(q(n)) = p(n) - 2\pi\tau V_1 \sin(2\pi q(n)) \\ q(n+1) &= q(n) + T'(p(n+1)) = q(n) + 2\pi\tau V_2 \sin(2\pi p(n+1))\end{aligned}$$

which with  $2\pi\tau V_i = \gamma_i$  answer the first question.

Plotting the iterates of the map in the square  $[0 : 1] \times [0 : 1]$  (the motion is periodic both in  $x$  and  $y$  directions with spatial periodicity 1) for some values of  $\gamma = \gamma_1 = \gamma_2$  one can recognize the transition to chaos typical of Hamiltonian systems. Indeed the behavior is not very dissimilar from that of the standard map, with the presence of KAM tori which get destroyed at increasing  $\gamma$  and with the persistency of regular islands also for large  $\gamma$  values.

## Exercise 7.4

*Consider the ODE*

$$\frac{dx}{dt} = -a(t) \frac{\partial \psi}{\partial y}, \quad \frac{dy}{dt} = a(t) \frac{\partial \psi}{\partial x}$$

where  $\psi = \psi(x, y)$  is a smooth function periodic on the square  $[0 : L] \times [0 : L]$  and  $a(t)$  an arbitrary bounded function. Show that the system is not chaotic.

### Solution

In order to prove that the system is non chaotic, we need to show that  $\psi$  is a conserved quantity for any  $a(t)$ , indeed,

$$\frac{d\psi}{dt} = \frac{\partial\psi}{\partial x} \frac{dx}{dt} + \frac{\partial\psi}{\partial y} \frac{dy}{dt} = -\frac{\partial\psi}{\partial x} \left[ a(t) \frac{\partial\psi}{\partial y} \right] + \frac{\partial\psi}{\partial x} \left[ a(t) \frac{\partial\psi}{\partial x} \right] = 0$$

With the change of the time variable:  $\tau = \int_0^t ds a(s)$ , we obtain the new system of ODE

$$\begin{aligned} \frac{dx}{d\tau} &= -\frac{\partial\psi}{\partial y} \\ \frac{dy}{d\tau} &= \frac{\partial\psi}{\partial x} \end{aligned}$$

which is the an integrable system with zero Lyapunov exponent.

This result holds for arbitrary choices of  $a(t)$ , for example we can take  $a(t)$  as a chaotic signal, e.g. the evolution of one variable of the Lorenz model, notwithstanding the chaoticity of  $a(t)$  the evolution of  $(x(t), y(t))$  is not chaotic, i.e. there are not positive Lyapunov exponents and so two close initial conditions do not diverge.

### Exercise 7.5

Consider the system defined by the Hamiltonian

$$H(x, y) = U \sin x \sin y$$

which is integrable and draw some trajectories, you will see counter-rotating square vortices. Then consider a time-dependent perturbation of the following form

$$H(x, y, t) = U \sin(x + B \sin(\omega t)) \sin y$$

study the qualitative changes of the dynamics at varying  $B$  and  $\omega$ . You will recognize that now trajectories can travel in the  $x$ -direction, then fix  $B = 1/3$  and study the behavior of the diffusion coefficient  $D = \lim_{t \rightarrow \infty} \frac{1}{2t} \langle (x(t) - x(0))^2 \rangle$  as a function of  $\omega$ . This system can be seen as a two-dimensional model for the motion of particles in a convective flow [Solomon and Gollub (1988)]. Compare your findings with those reported in Sec.11.2.2.2 (See also Castiglione et al. (1999)).

**Exercise 7.6**

Consider a variant of the Hénon-Heiles system defined by the potential energy

$$V(q_1, q_2) = \frac{q_1^2}{2} + \frac{q_2^2}{2} + q_1^4 q_2 - \frac{q_2^3}{3}.$$

Identify the stationary points of  $V(q_1, q_2)$  and their nature. Write the Hamilton equations and integrate numerically the trajectory for  $E = 0.06$ ,  $q_1(0) = -0.1$ ,  $q_2(0) = -0.2$ ,  $p_1(0) = -0.05$ . Construct and interpret the Poincaré section on the plane  $q_1 = 0$ , by plotting  $q_2, p_2$  when  $p_1 > 0$ .

## CHAPTER 8: Chaos and Information Theory

### Exercise 8.1

Compute the topological and the Kolmogorov-Sinai entropy of the map defined in Ex.5.12 using as a partition the intervals of definition of the map.

### Solution

Denote with  $N_n^{(1)}$ ,  $N_n^{(2)}$  and  $N_n^{(3)}$ , the number of sequences of length  $n$  ending with 1,2,3 respectively. The map of Ex.5.12 corresponds to a Markov chain represented in Fig.14, thus we can write the iteration law for  $N_n^{(1)}$ ,  $N_n^{(2)}$  and  $N_n^{(3)}$ ,

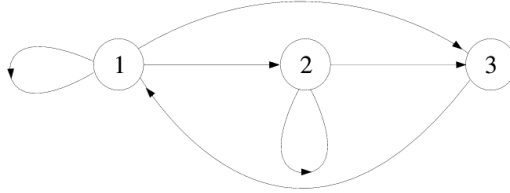


FIG. 14: Graphical representation of the MC associated to the considered map with the Markov partition, see Ex. 5.12.

$$N_{n+1}^{(1)} = N_n^{(1)} + N_n^{(3)}$$

$$N_{n+1}^{(2)} = N_n^{(1)} + N_n^{(2)}$$

$$N_{n+1}^{(3)} = N_n^{(1)} + N_n^{(2)}$$

Since  $N_1^{(1)} = N_1^{(2)} = N_1^{(3)} = 1$ , we have the solution

$$N_n^{(1)} = N_n^{(2)} = N_n^{(3)} = 2^{n-1}$$

The total number of admissible sequences of length  $n$  is

$$N_n^T = N_n^{(1)} + N_n^{(2)} + N_n^{(3)} = \frac{3}{2}2^n$$

implying that the topological entropy

$$h_{top} = \lim_{n \rightarrow \infty} \frac{1}{n} \ln N_n^T = \ln 2$$

The KS entropy is equal to the Lyapunov exponent computed in Ex. 5.12. To verify it one can also use the formula for computing the Shannon entropy associated to a Markov Chain, i.e. if  $\mathbb{W}$  is the  $M \times M$  transition matrix

$$h_{Sh} = - \sum_{i=0}^{M-1} p_i \sum_{j=0}^{M-1} \mathbb{W}_{ji} \ln \mathbb{W}_{ji},$$

where  $(p_0, \dots, p_{M-1}) = \mathbf{p}$  denotes the invariant probabilities, i.e.  $\mathbb{W}\mathbf{p} = \mathbf{p}$ , which were computed in Ex. 5.12.

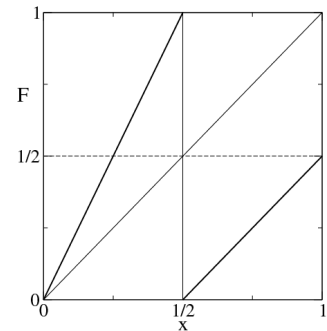
**Exercise 8.2**

Consider the one-dimensional map defined by the equation:

$$x(t+1) = \begin{cases} 2x(t) & x(t) \in [0:1/2) \\ x(t) - 1/2 & x(t) \in [1/2:1] \end{cases}$$

and the partition  $A_0 = [0:1/2]$ ,  $A_1 = [1/2:1]$ , which is a Markov and generating partition. Compute:

- (1) the topological entropy;
- (2) the KS entropy.



**Solution**

The partition  $[0:1/2[ [1/2:1]$  defines a Markov partition, characterized by the transition matrix

$$\mathbb{W} = \begin{pmatrix} 1/2 & 1 \\ 1/2 & 0 \end{pmatrix}$$

graphically represented in Fig.15.



FIG. 15:

1) Let us start computing the topological entropy.

Note that the  $k$ -words  $W_k$  ending with the symbol “1” generate a  $(k + 1)$ -word  $W_{k+1}$  such that  $i_{k+1} = 0$ , while a  $W_k$  ending with “0” generates  $W_{k+1}$  with  $i_{k+1} = 0$  or  $i_{k+1} = 1$ . Similarly to the previous exercise, denote with  $N_k^{(0)}$  and  $N_k^{(1)}$  the number of  $k$ -word ending with “0” and “1” respectively. One can easily find the recursion rule, we have

$$N_k^{(0)} = N_{k-1}^{(0)} + N_{k-1}^{(1)} = N_{k-1} \quad (12)$$

$$N_k^{(1)} = N_{k-1}^{(0)} = N_{k-1} \quad (13)$$

where  $N_k = N_k^{(0)} + N_k^{(1)} = N_{k-1} + N_{k-2}$ , which is nothing but the Fibonacci’s sequence and for large  $k$ , is known to diverge as

$$N_k \sim \mathcal{G}^k, \quad \text{with } \mathcal{G} = \frac{1 + \sqrt{5}}{2}$$

therefore

$$h_{Top} = \lim_{k \rightarrow \infty} \frac{\ln N_k}{k} = \ln \mathcal{G} = 0.481211825059603$$

b) The KS-entropy of this map is nothing but the Shannon entropy of the associated Markov Chain. The invariant probability of the Markov Chain is can be easily found. Denoting with  $P_0^{inv}$  and  $P_1^{inv}$  the invariant probability of the set  $A_0$  and  $A_1$  respectively, we have

$$P_0^{inv} = \frac{1}{2} P_0^{inv} + P_1^{inv} \quad (14)$$

$$P_1^{inv} = \frac{1}{2} P_0^{inv} \quad (15)$$

which solved gives  $(P_0^{inv}, P_1^{inv}) = (2/3, 1/3)$ . Using the formula

$$h_{Sh} = - \sum_{i=0}^1 P_i^{inv} \sum_{j=0}^{M-1} \mathbb{W}_{ji} \ln \mathbb{W}_{ji},$$

we find

$$h_{KS} = P_0^{inv} \ln(2) + P_1^{inv} \ln(1) = \frac{2}{3} \ln(2).$$

The condition  $h_{Top} > h_{KS}$  implies that the number of admitted words is much larger than the number of typical sequences  $N_k \gg N_k^{eff} \sim \exp(kh_{KS})$ .

From Ex 8.1 and 8.3, it is easy to find the general rule for the computation of all possible sequences of lenght  $n$  of a given partition. Denoting by  $\mathbf{N}_k$  the vector with components  $N_k^0, N_k^1, \dots$ , we can write

$$\mathbf{N}_k = A \mathbf{N}_{k-1}$$

where the entries of matrix  $A$  are 0 or 1, therefore  $N_k \sim a^k$ , being  $a$  the maximal eigenvalue of  $A$ , so that  $h_{Top} = \ln a$ . Of course, the above formula holds only for ergodic Markov chains.

### Exercise 8.3

Compute the topological and the Kolmogorov-Sinai entropy of the roof map defined in Ex.4.10 using the partitions: (1)  $[0:1/2[$ ,  $[1/2:1[$  and (2)  $[0:x_1[$ ,  $[x_1:1/2[$ ,  $[1/2:x_2[$ ,  $[x_2:1[$ . Is the result the same? If yes or not explain why.

### Hints and Solution

Notice that the second partition is a Markov partition and is a refinement of the first partition, which is a generating partition. Hence, also the Markov partition is generating and bring the same information. One can compute the topological and KS-entropy in the latter using the strategies defined in the previous two exercises.

### Exercise 8.4

Consider the one-dimensional map

$$x(t+1) = \begin{cases} 8x(t) & 0 \leq x < 1/8 \\ 1 - 8/7(x(t) - 1/8) & 1/8 \leq x \leq 1 \end{cases}$$

Compute the Shannon entropy of the symbolic sequences obtained using the family of partitions  $A_i^{(k)} = \{x_i^{(k)} \leq x < x_{i+1}^{(k)}\}$ , with  $x_{i+1}^{(k)} = x_i^{(k)} + 2^{-k}$ , use  $k = 1, 2, 3, 4, \dots$ . How does the entropy depend on  $k$ ? Explain what does happen for  $k \geq 3$ . Compare the result with the Lyapunov exponent of the map and determine for which partitions the Shannon entropy equals the Kolmogorov-Sinai entropy of the map.

### Hints and Solution

Notice that the partition  $[0:1/8[$  and  $[1/8:1[$  is generating and is a Markov partition. So that everything can be computed easily with such a partition. Clearly, for  $k \geq 3$  the resulting partition is a refinement of the generating partition and thus the Shannon entropy of the resulting sequences should be equal to the KS-entropy of the map, which in turn can be computed from the Markov partition. It remains to compute the Shannon entropy for  $k = 1, 2$ , from its definition we know that the KS-entropy is maximal over all possible partition. Thus for  $k = 1, 2$  either the Shannon entropy is equal to the KS-entropy or it is

smaller than it. Since these two partitions are not generating we expect that the resulting Shannon entropy is smaller. You can verify it numerically.

### Exercise 8.5

*Numerically compute the Shannon and topological entropy of the symbolic sequences obtained from the tent map using the partition  $[0:z[$  and  $[z:1]$  varying  $z \in ]0:1[$ . Plot the results as a function of  $z$ . For which value of  $z$  does the Shannon entropy coincide the KS-entropy of the tent map? and why?*

### Hints and Solution

When  $z = 1/2$  the partition is both generating and Markov. Clearly, for such a value the Shannon entropy should coincide with the KS-entropy.

### Exercise 8.6

*Numerically compute the Shannon entropy for the logistic map at  $r = 4$  using a  $\varepsilon$ -partition obtained dividing the unit interval in equal intervals of size  $\varepsilon = 1/N$ . Check the convergence of the entropy changing  $N$ , compare the results when  $N$  is odd or even, and explain the difference if any. Finally compare with the Lyapunov exponent.*

### Hints and Solution

For  $N = 2$ , the partition is generating. For  $N$  even the resulting partition is a refinement of a generating partition, and consequently is generating. Therefore, for any  $N$  even the entropy should be equal to the KS-entropy. On the other hand, at increasing  $N$  odd we should expect that the Shannon entropy should approximate better and better the KS-entropy.

### Exercise 8.7

*Numerically estimate the Kolmogorov-Sinai entropy  $h_{KS}$  of the Hénon map, for  $b = 0.3$  and  $a$  varying in the range  $[1.2, 1.4]$ , as a partition divide the portion of  $x$ -axis spanned by the attractor in sets  $A_i = \{(x, y) : x_i < x < x_{i+1}\}$ ,  $i = 1, \dots, N$ . Choose,  $x_1 = -1.34$ ,  $x_{i+1} = x_i + \Delta$ , with  $\Delta = 2.68/N$ . Observe above which values of  $N$  the entropy approach*



*the correct value, i.e. that given by the Lyapunov exponent.*

## CHAPTER 9: Coarse-grained information and large scale predictability

### Exercise 9.1

Consider the one-dimensional map  $x(t+1) = [x(t)] + F(x(t) - [x(t)])$  with

$$F(z) = \begin{cases} az & \text{if } 0 \leq z \leq 1/2 \\ 1 + a(z - 1) & \text{if } 1/2 < z \leq 1, \end{cases}$$

where  $a > 2$  and  $[..]$  denotes the integer part of a real number. This map produces a dynamics similar to a one-dimensional Random Walk. Following the method used to obtain Fig.B19.2, choose a value of  $a$ , compute the  $\varepsilon$ -entropy using the Grassberger-Procaccia and compare the result with a computation performed with the exit-times. Then, being the motion diffusive, compute the diffusion coefficient as a function of  $a$  and plot  $D(a)$  as a function of  $a$  (see Klages et al 1995). Is it a smooth curve?

### Hints and Solution

When using the GP method one needs to change the sampling time, this problem is not present with exit time method. After having performed the computation of the entropy with a value of the parameter  $a$ , one can check the dependence of the diffusion coefficient on  $a$ . As reported in “Simple Maps with Fractal Diffusion Coefficients”, Phys. Rev. Lett. **74**, 387-390 (1995), the function  $D(a)$  is non smooth and fractal like.

### Exercise 9.2

Consider the one-dimensional intermittent map

$$x(t+1) = x(t) + ax^z(t) \pmod{1}$$

fix  $a = 1/2$  and  $z = 2.5$ . Look at the symbolic dynamics obtained by using the partition identified by the two branches of the map. Compute the  $N$ -block entropies as introduced in Chapter.8 and compare the result with that obtained using the exit-time  $\epsilon$ -entropy (Fig.B19.3b). Is there a way to implement the exit time idea with the symbolic dynamics obtained with this partition?

### Hints and Solution

With the proposed partition there will be long sequences of zeros, one possibility is to code such sequences in terms of their length, and thus compute their average length.

#### Exercise 9.3

*Compute the FSLE using both algorithms described in Fig.9.6 and Fig.9.7 for both the logistic maps ( $r = 4$ ) and the tent map. Is there any appreciable difference?*

### Hints and Solution

Be careful when using the first method to maintain the perturbed trajectory inside the unit interval. Anyway you should see some small differences only for large values of the perturbation.

#### Exercise 9.4

*Compute the FSLE for the generalized Bernoulli shift map  $F(x) = \beta x \pmod{1}$  at  $\beta = 1.01, 1.1, 1.5, 2$ . What does changes with  $\beta$ ?*

### Hints and Solution

You should observe that the nonlinear effects, which manifest with the presence of high values of  $\lambda(\delta)$  at finite  $\delta$  values are more evident when  $\beta$  is closer to 1.

#### Exercise 9.5

*Consider the two coupled Lorenz models as in Eq.(9.23) with the parameters as described in the text, compute the full Lyapunov spectrum  $\{\lambda_i\}_{i=1,6}$  and reproduce Fig.9.10.*

### Hints and Solution

This numerical exercise should not present any particular difficulty once you have well tested codes for computing the Lyapunov exponents and the FSLE, as required from previous exercises.